Differentially expressed genes associated with resistance to red palm weevil (Rhynchophorus ferrugineus) infestation in coconut (Cocos nucifera L.) and identification of rSNP markers in disease resistance genes

N. Umaa Malani
Universiti Putra Malaysia
Siti Nor Akmar Abdullah
snaa@upm.edu.my

Universiti Putra Malaysia
Norida Mazlan
Universiti Putra Malaysia

Research Article

Keywords: coconut, red palm weevil, RNA-seq, promoter SNP, resistance genes, transcriptomics

Posted Date: January 8th, 2026

DOI: https://doi.org/10.21203/rs.3.rs-7994557/v1

Additional Declarations: No competing interests reported.

Abstract

BACKGROUND

Red palm weevil (*Rhynchophorus ferrugineus*) is a major pest threatening coconut (*Cocos nucifera*) production worldwide. The hidden nature of larval feeding in the tree trunk hinders early detection. When visible symptoms appear, often it is already too late to save infested trees. Despite its economic importance, the molecular basis of host resistance to this invasive pest remains unclear. This study aimed to identify differentially expressed genes (DEGs) associated with resistance to red palm weevil (RPW) and develop gene-based single nucleotide polymorphic markers for coconut improvement.

RESULTS

Comprehensive assessment of internal and external damages of coconut trees in a heavily infested field identified Malayan Yellow Dwarf (MYD) as a resistant while Pandan and Malayan Tall (MT) as the susceptible coconut varieties. Illumina NovaSeq platform generated 150 bp paired ends reads from 18 cDNA libraries constructed using RNA from the leaves of these three coconut varieties from infested fields and non-infested fields (control). Differential expressed genes analysis by DESeq2 showed MYD had the greatest number of DEGs (4,314 upregulated and 4,469 downregulated), while Pandan had 1,999 upregulated and 1,660 downregulated and MT had 1,988 upregulated and 2,185 downregulated DEGs. Disease-resistance genes, including the *RGA1*, *RGA3* and *RPS2* were significantly upregulated in MYD. Genes encoding transcription factors (NAC, WRKY, MYB, ERF and CAMTA) as well as phytohormone signalling (jasmonic acid, salicylic acid and ethylene) and stress responsive (heat shock protein and hypersensitive response) genes exhibited highest expression levels in MYD and lower or undetectable in the Pandan and MT. Alignment of 3.0 kb of sequences upstream of the transcriptional start site in the DEGs encoding disease resistance genes from the different varieties identified SNP variants associated with differential response to RPW. Three significant SNP variants were identified in *RGA3* promoter region of the Pandan variety. These variants were found in the MYB-binding motif, TATA-box and CAAT-box.

COCLUSION

Collectively, our findings provide an integrated view of transcriptional and genetic variations linked to coconut resistance against RPW. The identified DEGs and variants within the *RGA3* promoter represent valuable markers to be used in marker assisted selection in breeding programs for developing RPW-resistant coconut varieties.

Background

The coconut palm (*Cocos nucifera* L.) is a perennial tropical crop of immense socio-economic importance, particularly across the Asia-Pacific region where it supports the livelihoods of millions of smallholders. As the sole species of the genus *Cocos* within the *Arecaceae* family, coconut exhibits extensive genetic diversity, with over 1,000 accessions conserved globally through the International Coconut Genebanks. Despite this diversity, the absence of a standardized molecular taxonomy continues to limit the efficiency of breeding programs (1). Coconut varieties are broadly categorized as tall (*typica*) or dwarf (*nana*) based on morphology and reproductive behaviour. Tall varieties, such as Malayan Tall (MT) and Tagnanan Tall, are cross-pollinated and long-lived with high copra yield, while dwarf types like Malayan Yellow Dwarf (MYD) and Pandan are self-pollinating and early bearing, preferred for tender nut production. Hybrids between these groups, such as MAWA (MYD × West African Tall) and MATAG (Malayan Dwarfs × Tagnanan Tall), combine high yield potential with disease tolerance and early fruiting (2). In Malaysia, coconut remains a key plantation crop, contributing to food security and rural livelihoods, with dwarf varieties such as MYD, Malayan Red Dwarf (MRD) and Pandan cultivated for diverse purposes (3).

However, the sustainability of coconut production is increasingly threatened by biotic and abiotic stresses, particularly infestations by the invasive red palm weevil (*Rhynchophorus ferrugineus*), one of the most destructive insect pests of palm species worldwide. Native to Southeast Asia, this pest has now spread to more than 49 countries across Asia, Africa, and Europe (4). The larvae bore deep into the trunk, feeding on soft tissues, disrupting vascular transport, and eventually killing the palm within months (5). In Malaysia, the first confirmed outbreak occurred in Terengganu in 2007, and infestations have since expanded across all districts, severely affecting smallholder income and replanting efforts (6). The concealed nature of larval feeding makes early detection extremely difficult, with visible symptoms such as wilting, trunk holes, foul odour, and apical death only appearing during advanced stages. Current management practices, including pheromone trapping, insecticide application, and biological control, have provided limited and costly protection (7, 8). Although recent advances in acoustic, imaging, and deep learning-based detection methods show promise, their adoption remains restricted due to high costs and technical constraints (9).

Host-plant resistance represents the most sustainable and environmentally friendly strategy for controlling RPW infestation. However, limited information is available on the molecular basis of resistance among coconut varieties. Preliminary field observations suggest that MYD exhibits tolerance to RPW, whereas Pandan and MT are more susceptible (10). Biochemical studies have shown that resistant genotypes maintain stronger antioxidant systems and elevated defence responses compared to susceptible ones (11). These findings suggest that genetic and transcriptional regulation play key roles in determining resistance levels, yet the specific genes and regulatory elements involved remain largely unknown.

Plants employ a multifaceted defence system involving structural barriers, signalling molecules, and secondary metabolites that collectively protect against herbivory (12). Defence mechanisms are typically mediated through two immune responses: pattern-triggered immunity (PTI) and effector-triggered

immunity (ETI) (13). PTI involves early pathogen recognition through pattern-recognition receptors, activating defence-related transcription factors and secondary metabolite production (14). ETI, mediated by resistance (R) genes such as nucleotide-binding leucine-rich repeat (NLR) proteins, triggers localized cell death and systemic acquired resistance (15). Resistance gene analogues (RGAs) and ribosomal protein S2 (RPS2) homologs have been identified in various crops as key regulators of pest resistance (16). In coconut, several putative R-genes have been annotated from genome sequences (17) but their functional roles in pest resistance, particularly against RPW, have not been characterized.

The integration of transcriptomic and genomic approaches offers powerful tools to dissect plant-pest interactions. RNA sequencing (RNA-seq) enables genome-wide identification of differentially expressed genes (DEGs) under stress conditions, revealing the molecular pathways that underpin resistance mechanisms (18). Previous transcriptomic studies in coconut have focused primarily on diseases such as *Phytophthora palmivora* and phytoplasma (19, 20) but equivalent research on insect-induced responses remains limited. Complementary to transcriptomics, whole-genome resequencing allows detection of single nucleotide polymorphisms (SNPs), providing high-resolution markers linked to resistance traits (21). SNPs located in gene promoter regions are particularly valuable, as they can alter transcription factor binding motifs (e.g., TATA-box, CAAT-box, and MYB sites), influencing gene expression and defence activation (22). The recent availability of high-quality reference genomes for tall and dwarf coconut varieties (23, 24) now facilitates precise detection of such regulatory polymorphisms.

Despite the recent availability of high-quality coconut reference genome, little information exists on the transcriptional data and promoter variation associated with resistance to *R. ferrugineus* to understand the molecular responses. Hence, this study aimed to fill this knowledge gap by phenotypic characterization of the resistant and susceptible varieties and identifying DEGs and GO enriched pathways associated with RPW tolerance using RNA-seq. The study hoped to produce potential molecular markers associated with RPW resistance through identification of functional SNPs within the regulatory regions of the differentially expressed disease-resistant genes.

Material and Methods

Plant materials and sample collection

Phenotypic characterization was performed on 20-year-old mature coconut palms from three varieties: MYD, Pandan, and MT. The samples were collected from a field naturally infested with RPW at Pantai Batu Burok, Kuala Terengganu, Malaysia (Latitude: 5.311750, Longitude: 103.160111). Two non-infested control locations were selected: Pusat Pertanian Lekir, Perak (Latitude: 4.1379° N, Longitude: 100.7320° E) and Pusat Pertanian Teluk Bahru, Perak (Latitude: 3.8903° N, Longitude: 100.8975° E). All plant materials were formally identified by the Science Officer, Department of Agriculture, Marang, and voucher specimens were deposited at NCBI under BioProject: PRJNA1375459. Collection of plant material complied with institutional and national guidelines, and permission for sample collection from field-grown palms was obtained from the respective authorities.

Eighteen young leaf samples were collected for transcriptome analysis following characterization of symptoms in RPW infested field. The samples included both naturally infested and healthy palms from non-infested field from three varieties of coconut, each with three biological replicates, as detailed in Table 1. A total of nine samples were collected from infested palms located at Pantai Batu Burok in Terengganu, alongside nine samples from non-infested palms at Pusat Pertanian Lekir and Teluk Bahru in Perak. The control palms exhibited no apparent signs of RPW attack, functioning as a healthy benchmark for comparative analysis.

Table 1
Treatment and control groups used for RNA-seq analysis.

Comparison	Treatment group	Control group
1	FPI	FPC
2	FMTI	FMTC
3	FMYDI	FMYDC

FPI, FMTI and FMYDI represent Pandan, Malayan Tall and Malayan Yellow Dwarf from infested field, respectively. FPC, FMTC and FMYDC represent Pandan, Malayan Tall and Malayan Yellow Dwarf from non-infested field, respectively that served as control.

Twenty-seven spear leaf samples were obtained from three varieties: Pandan (11 accessions), MYD (8 accessions), and MT (8 accessions) for promoter analysis of selected disease resistance DEGs. Samples were collected from RPW infested palms at Pantai Batu Burok, Terengganu, and from healthy, non-infested palms at Pusat Pertanian Lekir and Teluk Bahru, Perak. Selection was based on the phenotypic characterization that categorized palms as control, low-infested, or high-infested to encompass genetic diversity across infestation levels (Additional file 1). Genomic DNA obtained from these samples was utilized to identify variants in the promoter regions of disease-resistance genes potentially linked to resistance against the RPW.

Phenotypic characterization of RPW infestation symptoms and damage

A field phenotypic characterization was carried out to identify both external and internal symptoms associated with *Rhynchophorus ferrugineus* infestation in three coconut varieties: MYD which represents the tolerant with Pandan and MT representing the susceptible categories. Palms were observed in their natural field environment for a duration of four months. External symptoms including trunk holes, frond wilting, leaf discolouration, and crown collapse were assessed using a descriptive scale ranging from 0 to 3, reflecting a progression from no damage to complete plant death in Table 2.

Palms exhibiting significant external symptoms (score 3) were assessed for internal damage. Inspections were conducted on the cross-sections of the trunk and cabbage region to identify the presence of tunnels, larvae, pupae, and adult weevils. Five palms demonstrating significant infestation were chosen for comprehensive internal evaluation. The findings revealed significant tissue damage along with various developmental stages of RPW, indicating a notable level of susceptibility. Due to the qualitative nature of the traits, the results are conveyed through descriptive comparisons among the varieties instead of through statistical analyses.

Table 2
Infestation level and its corresponding symptoms.

Infestation Level	Symptoms
No infestation (Level 0)	• No holes in trunk/petiole • Healthy apical shoot • No frond collapse or wilting • Minimal or no dried leaves • Healthy crown appearance • No oozing of sap
Low infestation (Level 1)	• Minor physical damage observed • Presence of 1–2 holes in trunk/petiole • Healthy apical shoot • Minimal frond collapse • Few dried leaves • Healthy crown appearance • No oozing of sap
Medium infestation (Level 2)	• Moderate physical damage observed • Presence of 3–6 holes in trunk/petiole • Apical shoot slightly damaged • Slight frond collapse or wilting • Moderate number of dried leaves • Crown remains partially healthy • Occasional oozing of sap (thick fluid)
High infestation (Level 3)	• Severe physical damage observed • Presence of > 6 holes in trunk/petiole • Apical shoot severely damaged or dead • Extensive frond collapse or wilting • Majority/all leaves dried • Crown fully damaged or collapsed • Visible oozing of sap (thick, foul-smelling fluid)

RNA Extraction and mRNA Library Construction

RNA was extracted from 200 mg of frozen leaf tissue utilizing the SEPa Plant RNA Isolation Reagent Kit (1st BASE, Singapore), adhering to a modified lithium chloride (LiCl) precipitation protocol (20). After washing with 70% ethanol the RNA pellets were dissolved in RNase-free water. The DNase module of the kit was employed to eliminate DNA contamination. The assessment of RNA quantity and purity was conducted using a NanoDrop spectrophotometer, while integrity was confirmed through agarose gel electrophoresis and analysis with an Agilent 2100 Bioanalyzer. Samples were selected for library construction based on an RIN of 7 or higher and a 28S:18S ratio of 1.5 or greater.

Messenger RNA (mRNA) was isolated through the use of oligo(dT) magnetic beads and subsequently fragmented before the synthesis of cDNA. Libraries specific to each strand were constructed through the incorporation of dUTP during the synthesis of the second strand. This process was subsequently followed by the ligation of adapters, amplification via PCR, and selection based on size. The quality of the library was validated using Qubit, qPCR, and Bioanalyzer assays. Sequencing was conducted at NovogeneAIT Genomics in Singapore using the Illumina NovaSeq X Plus platform, resulting in paired-end reads of 150 bp. Following the removal of adapters and low-quality reads with FastQC v0.11.9, high-quality clean reads was retained for subsequent analyses.

Read alignment and identification of differentially expressed genes

Clean reads were aligned to the *Cocos nucifera* reference genome (Accession: GWHBEBU00000000; https://ngdc.cncb.ac.cn/gwh/Assembly/21822/show) utilizing HISAT2 v2.0.5 following the construction of the index. Transcript assembly was conducted using StringTie version 1.3.3b, while raw read counts were obtained through FeatureCounts version 1.5.0. The normalization of gene expression levels was conducted utilizing the DESeq2 package (v1.38.2) within the R programming environment. Genes exhibiting |log2 fold change| ≥ 1 and an adjusted p-value (FDR) ≤ 0.05 were identified as differentially expressed. Genes that were upregulated exhibited increased expression levels in infested palms in comparison to the control group, whereas downregulated genes demonstrated a decrease in expression.

Gene Ontology (GO) enrichment analysis

The functional enrichment analysis of DEGs was conducted utilizing clusterProfiler (v4.8). We identified significantly over-represented Gene Ontology (GO) terms in biological process (BP), molecular function (MF), and cellular component (CC) categories, with a false discovery rate (FDR) of less than 0.05, while accounting for gene length bias. We visualized enriched GO categories using bar and bubble plots to emphasize the significant pathways linked to defense and stress response mechanisms.

DNA synthesis and quantitative real-time PCR (qRT-PCR) validation

RNA from all 18 samples (three varieties × treatment and control) was treated with DNase and subsequently reverse-transcribed into cDNA using the RevertAid First Strand cDNA Synthesis Kit (Thermo Fisher Scientific, USA), adhering to the manufacturer's guidelines. About 600 ng of cDNA was generated for each reaction and preserved at − 80°C for future analyses. Quantitative real-time PCR (qRT-PCR) was employed to confirm the expression levels of specific differentially expressed genes that were identified through RNA sequencing. Primers specific to the genes were developed utilizing Primer3 v4.1.0 (Additional file 2). The reactions, totalling 10 µL in volume, comprised 1× Maxima SYBR Green Master Mix (Thermo Fisher Scientific, USA), 0.2 µM of each primer, and 9 ng of cDNA template. Amplifications were conducted using a Bio-Rad CFX384 Touch Real-Time PCR System with the following parameters: an initial denaturation at 95°C for 1 minute, succeeded by 40 cycles consisting of 95°C for 15 seconds and a primer-specific annealing step lasting 30 seconds. Melt-curve analysis conducted within the temperature range of 65 to 95°C, with increments of 0.5°C, validated the specificity of the amplicon.

The normalization of relative expression was conducted utilizing two validated reference genes, CneIF-4γ and CnEF-1α (25). CnEF-1α and CneIF-4γ were chosen as reference genes due to their stable expression across biotic and hormone-induced stress conditions in coconut, ensuring accurate normalization of RT-qPCR data. The evaluation of statistical significance was conducted using one-way ANOVA followed by Tukey's post hoc test (SPSS). The expression data are reported as mean ± SEM, based on three biological replicates.

SNP discovery from whole genome resequencing data

Seventeen candidate disease-resistance genes identified from transcriptomic analysis were selected for promoter-region variant screening using data from whole-genome resequencing of 27 leaf samples representing three coconut varieties Pandan, MYD, and MT collected from both *Rhynchophorus ferrugineus* infested and non-infested fields. High-quality reads were aligned to the *Cocos nucifera* reference genome, and SNPs were called and filtered for quality. Comparative analyses were conducted for three pairwise groups: MYD vs. Pandan, MYD vs. MT and MT vs. Pandan. Significant allele-frequency differences were identified using Fisher's exact test with false-discovery-rate (FDR) correction. FDR employed to identify genotype–phenotype associations due to its efficacy in managing small datasets and categorical distributions. SNPs situated within 3-kilobase promoter region upstream of the transcriptional start site that coincide with established cis-regulatory motifs were designated as putative functional variants that may affect gene expression.

SNP variant calling in promoter regions

Variant discovery was confined to 3.0 kb upstream of transcription start sites of 17 disease-resistance genes identified from transcriptomic data (Additional file 3). Promoter coordinates were established using BEDTools, and SNPs were identified with GATK HaplotypeCaller v4.4. Variants were refined

utilizing GATK VariantFiltration with the following criteria: QD > 2.0, QUAL > 30, FS < 60, SOR < 3, MQ > 40, MQRankSum > − 12.5, and ReadPosRankSum > − 8. Filtered VCFs were compressed, indexed, and amalgamated using bcftools to generate a consolidated dataset for subsequent analyses.

Comparative analysis of SNPs among varieties

Pairwise SNP comparisons were conducted among Pandan, MYD, and MT varieties. Custom Python scripts filtered and identified SNPs unique to each comparison group (MYD vs Pandan, MYD vs MT, and MT vs Pandan). Variety-specific variants were extracted into separate VCF files for further annotation and statistical analysis.

Variant annotation and visualization

A bespoke SnpEff v5.1 database for coconut was constructed by amalgamating the genome and GFF annotation files. Annotated VCFs and summary reports (gene and HTML files) were produced for each comparison. Heatmaps were employed to visualize the distribution of significant SNPs, demonstrating genotype clustering between resistant and susceptible varieties.

Statistical analysis of SNP variants

FDR was utilized for each SNP to evaluate the correlation between allele presence and resistance phenotype. P-values were adjusted for multiple comparisons utilizing the Benjamini–Hochberg false discovery rate method; variants with an FDR < 0.05 were deemed significant. Analyses were conducted utilizing Python scripts to produce 2 × 2 contingency tables that compare resistant and susceptible groups (supplementary data)

Annotation of promoter motifs for significant SNPs

The promoter sequences of the 17 candidate genes were extracted using BEDTools getfasta and analyzed for cis-regulatory motif prediction via the PlantCARE database. SNP positions in BED format were intersected with motif coordinates utilizing BEDTools intersect to identify variants that overlap with regulatory motifs. Single nucleotide polymorphisms within motifs were regarded as putative regulatory markers that may affect gene expression associated with resistance to the RPW.

Results

Phenotypic characterization of external damage of the palm

Phenotypic characterization examining RPW infestation symptoms across the three coconut varieties (MT, Pandan, and MYD) focusing on external damage was performed based on Table 2. Most Pandan and MT palms showed moderate to severe damage (Levels 2–3), including multiple trunk holes, collapsed fronds, drying leaves and damaged crowns. In contrast, MYD palms exhibited only mild

symptoms (Level 1), such as a few holes, drying leaves while maintaining healthy crowns and apical shoots.

The severely damaged Pandan (Level 3) symptoms of RPW infestation include numerous trunk holes, a severely damaged apical shoot, complete collapsed fronds, widespread leaf drying and a fully collapsed crown, indicating a high level of infestation (Fig. 1A ad 1B). These observations reflect the high vulnerability of the Pandan variety. Similarly, the MT variety displayed extensive (Level 3) structural and physiological damage. Severely infested palms had six or more trunk holes, destroyed apical shoots, wilting, collapsed fronds, desiccated leaves, and fully damaged crowns (Fig. 1C and 1D). These symptoms confirm that MT is another susceptible variety prone to severe RPW damage.

In contrast, most of MYD palms were either symptom-free (Level 0) or exhibited low-level symptoms (Level 1), such as more than three holes, some dried leaves, and slight frond collapse, while maintaining healthy apical shoots and crowns appearance (Fig. 1E and 1F). These findings suggest that the MYD variety is more resistant to RPW infestation.

Phenotypic characterization of internal damage of the palm

Both MT and Pandan varieties that exhibited Level 3 RPW infestation, were characterized by severe internal damage. The MT variety as shown in (Fig. 2) showed severe internal deterioration, with blackened cabbage tissue, trunk tunneling, and chewed petiole fibers. High larvae and RPW presence were observed, often accompanied by a foul smell. Notably, MT showed signs of infestation starting at the base of the trunk, with tunneling progressing upward to the cabbage. Similarly, in the Pandan variety (Fig. 3), RPW larvae fed extensively on the internal cabbage, destroying fibers and hollowing out tissues, which led to palm collapse from within before visible external symptoms appeared. The cabbage tissues were chewed and tunneled through, resulting in blackened, decaying areas with a foul odor, and numerous pupal cases and larvae were found in the petiole, where eggs had been deposited. These findings confirm that both varieties are highly susceptible to RPW, suffering extensive structural and physiological damage that often remains hidden until advanced infestation.

To ensure similar environmental exposure, this study collected leave samples from MT, Pandan, and MYD coconut cultivars under equal field conditions. RPW infestation caused level 2 damage to MT and Pandan, with three biological replicates examined for transcriptomics. Due to plant degeneration and mortality, level 3 damage samples could not be collected. Pandan and MT had no field damage level 1 palms. MYD showed only level 1 damage, suggesting a physiological or genetic basis for its resistance. The observed differences suggest that inherent genetic variables affect the variety's ability to manage RPW-induced stress. We hypothesize that Pandan and MT are susceptible to RPW due to the severity of the damage, while MYD is more resistant due to the least palm damage in the same infested field.

Comparative transcriptomics of susceptible and resistant varieties under RPW infestation

Transcriptome sequencing using the Illumina NovaSeq X Plus (Illumina, USA) at Novogene, Singapore of 18 leave samples yielded 720,702,000 properly mapped paired-end clean reads, with 356,495,172 reads in control samples and 364,206,828 reads in infested samples. Among all the sequenced reads, 91.73%-89.4% were successfully and properly mapped to the reference genome, with an average of 90.50%. The unmapped reads were then excluded from further analysis. The average error rates, Q20%, and guanine-cytosine content were 0.01, 98.64%, and 48.92%. Figure 4 shows that Pandan reported 115,457,742 (control) and 116,819,824 (infested) read counts for each variety, a log2 fold change of 0.0156. MYD recorded 120,168,520 (control) and 122,346,128 (infested) with 0.03 log2 fold change. MT had 119,506,828 (control) and 126,402,958 (infested) with the highest log2 fold change of 0.08 (Additional file 4). The constant read counts and fold variations across biological replicates enable strong identification of stress-related DEGs, revealing resistance mechanisms in the three coconut varieties.

The mRNA fragments (150 bp) were generated from the FastQC analysis which employs Phred base calling as a metric to evaluate the base call quality across the sequenced reads. The mean quality (represented by the blue line) fell to the green region's scores of 38–40, which denotes very good quality calls as shown in Fig. 5. The obtained clean paired-end reads were mapped to the *Cocos Nucifera* reference genome (23) using the HISAT tool.

MYD showed the highest count of unique genes among the upregulated DEGs, totalling 4,314 (42.1%), reflecting significant transcriptional activation due to infestation. MT had 1,988 unique DEGs (27.6%), whereas Pandan recorded the lowest at 1,999 (13.9%). Commonly upregulated DEGs among the varieties included 207 genes (2.0%) shared by all three. MYD exhibited the highest count of unique downregulated DEGs, totalling 4,469, which represents 36%, indicating a dynamic regulatory response. MT exhibited 2,158 unique downregulated DEGs, accounting for 25%, while Pandan showed 1,660, representing 13.7%. Just 156 genes (1.4%) were consistently downregulated in all varieties. MYD showed the most significant transcriptional changes in gene activation and repression, suggesting a more adaptive and responsive defense mechanism against RPW stress than the other two varieties (Fig. 6).

GO Analysis

The findings from the Gene Ontology (GO) enrichment analysis for the three coconut varieties Pandan, MYD, and MT are presented in Table 3. The table outlines the number of enriched GO terms for each variety and regulation type (upregulated or downregulated), along with the total genes associated, the count of significantly enriched pathways, and the specific genes involved in these pathways across the three primary GO categories: Biological Process (BP), Cellular Component (CC), and Molecular Function (MF).

Table 3
The number of enriched GO terms, total genes, and significant pathways (with genes in significant pathways) for each cluster

Cluster	Pandan	MYD	MT
UP BP	409 / 2856 / 24 (282)	483 / 5471 / 0 (0)	444 / 4056 / 21 (679)
UP CC	107 / 498 / 0 (0)	125 / 943 / 0 (0)	123 / 1222 / 30 (581)
UP MF	285 / 2314 / 3 (27)	316 / 4106 / 14 (406)	306 / 2702 / 18 (500)
DW BP	415 / 2994 / 1 (23)	493 / 6545 / 21 (1051)	454 / 3229 / 1 (20)
DW CC	91 / 640 / 8 (141)	128 / 1459 / 8 (670)	104 / 671 / 10 (141)
DW MF	263 / 2007 / 3 (83)	313 / 4509 / 25 (1356)	293 / 2315 / 14 (575)

GO, Gene Ontology; BP, Biological Process; CC, Cellular Component; MF, Molecular Function; UP, up-regulated; DW, down-regulated; MYD, Malayan Yellow Dwarf; MT, Malayan Tall. GO enrichment analysis was performed using standard thresholds ($P < 0.05$). Results are formatted as *Enriched GO Terms / Total Genes / Significant Pathways (Genes in Significant Pathways)*. Numbers in parentheses indicate the number of genes associated with significant pathways within each category.

As shown in Fig. 7A, Pandan exhibited notable enrichment of metabolic and photosynthetic pathways, with genes that were upregulated related to trehalose synthesis and RNA glycosylase function. Upregulated RNA glycosylase activity indicates enhanced RNA surveillance that supports defense gene expression by eliminating damaged or pathogenic RNA molecules during pest stress, whereas downregulated genes were associated with photosynthesis and thylakoid activities (Additional file 5). Figure 7B shows MYD showed a reduced number of enriched pathways in the upregulated genes, highlighting significant roles in ADP binding, ATPase activity, and ion channel regulation. In contrast, there was a wider array of enriched processes observed in the downregulated genes, especially concerning translation, peptide biosynthesis, and ribosomal functions (Additional file 6). In MT, as shown in Fig. 7C, analysis revealed a variety of enriched pathways among both upregulated and downregulated genes. The upregulated genes prominently featured pathways related to vesicle-mediated transport, protein localization, and membrane processes, whereas the downregulated genes were associated with photosynthesis, thylakoid functions, and transcription regulation (Additional file 7).

The heatmap in Fig. 8 for top 100 upregulated genes, shows expression of a wide range of genes that help the coconut palms resist disease and respond to stress.

A variety of gene expression changes associated with disease resistance and stress responses were identified. The biological samples showing increased expression of immune response genes, especially those in green and yellow tones, are likely associated with the MYD coconut variety, known for its strong resistance to RPW infestation. The genes RGA1_SOLBU, RGA3_SOLBU, and DRL37_ARATH show significant elevation in MYD, encoding disease-resistance proteins featuring NB-ARC and RxN-terminal

domains. The prevalence of RGA3_SOLBU in the dataset suggests the presence of distinct isoforms or splicing variants. RPS2 expression is notably higher in MYD than in Pandan or MT, highlighting its unique role in pathogen recognition and defence signaling.

Alongside R genes, various transcription factors and signalling components were identified as differentially expressed. WRKY23, WRKY33, and WRKY70, together with NAC-domain transcription factors, are crucial in modulating immune gene expression and augmenting subsequent defences upon pathogen recognition. The GATA-type transcription factor GAT21_ARATH and the rice-derived kinase PTI0_ORYSJ, associated with PAMP-triggered immunity (PTI), exhibited increased expression. Similarly, MAPK3_ARATH, a Mitogen-Activated Protein Kinase, was positioned inside the top 100 genes in MYD and has a crucial upstream function in hormone signaling, reactive oxygen species (ROS) production, and cell wall reinforcement (27). Genes associated with cell wall modification, including CAD-C, CAD-D, and CADH_POPDE downstream in the MAPK3 pathway, exhibited elevated expression in MYD. These genes facilitate lignin production and cinnamyl alcohol dehydrogenase activity, hence strengthening the cell wall structure (28).

Furthermore, among the top 100 downregulated genes XTH1 and XTH8 in MYD impede cellulose degradation, thereby increasing cell wall rigidity alongside other with other downregulated genes such as endoglucanase 24 and Os09g0533900. A more pronounced downregulation of XTH25, which relaxes cell wall constituents (29), further substantiates the notion that MYD fortifies structural defenses against RPW larvae penetration. Likewise, SUS1_TULGE, a sucrose synthase gene, exhibited a more pronounced downregulation in MYD compared to Pandan and MT, indicating a strategic decrease in sugar availability that may limit pathogen access to nutrients (30).

Hormonal signalling pathways were significantly active in MYD. MAPK3_ARATH and TMK1 not only enhanced cell wall fortification but also had a role in hormone signalling. The ethylene signalling system exhibited activation, notably via the downregulation of CTR1, a high-affinity copper absorption gene that typically inhibits ethylene responses (31). Our data also showed that genes associated with brassinosteroid signalling, including BZR1 and P450 85A1, were increased in MYD, reinforcing the balance between growth and defence as well as immunological activation (32).

In the JA and ET signalling domains, numerous key genes exhibited differential expression. JAMYB_ORYSJ, which governs JA-dependent secondary metabolite synthesis, ranked among the top 100 most elevated genes in MYD. The increased expression of ACCO_MUSAC and OPR2_ARATH, pivotal genes in ethylene and jasmonic acid (JA) production respectively, strengthens the activation of these hormonal pathways. Concurrently, CHI, a chalcone isomerase integral to flavonoid biosynthesis, exhibited downregulation, indicating a reallocation of metabolic resources from flavonoid synthesis to jasmonate-mediated defences (33). This metabolic shift presumably facilitates improved JA responses to pest attack. In addition to this hormonal interaction, WRKY6_ARATH, WRKY75_ARATH and DRL13_ARATH which facilitate salicylic acid (SA) signalling, exhibited elevated expression in MYD, indicating the synchronised activation of many hormonal defence mechanisms.

The heatmap additionally features stress response genes, including BAG5_ARATH and DNJ1_CAEEL, which encode heat shock proteins that maintain protein stability during immunological responses (34). HSP82, an additional molecular chaperone, likewise stabilises immunological signalling proteins. DND1_CUCSA was produced to refine the hypersensitive response (HR), a crucial mechanism that mitigates excessive cellular apoptosis during immunological activation. Furthermore, genes from the glutathione S-transferase (GST) family, including GSTFC and GSTF3, were elevated in MYD, significantly contributing to reactive oxygen species (ROS) detoxification and the preservation of cellular redox equilibrium (35). Notably, At5g45910, which encodes a GDSL lipase, was downregulated in MYD, indicating diminished dependence on lipid-mediated signalling (36).

Transporter genes were another essential category that strengthened MYD's defensive capabilities. ABCB19_ARATH, a member of the ATP-binding cassette (ABC) transporter family, is among the top 100 upregulated genes in MYD and is recognized for its role in mediating auxin transport, therefore enabling hormonal crosstalk and defense coordination. Transporters such as NtABCG5, ABCB29, and UGT71, although not ranked among the top 100, were elevated and facilitate the movement of secondary metabolites and detoxification products (37). Conversely, the TAAC gene, responsible for the transport of 3'-phosphoadenosine 5'-phosphosulfate (PAPS) in glucosinolate production, exhibited downregulation, indicating a reallocation of ATP and metabolic resources towards more rapid defence responses [33].

Collectively, these findings demonstrate that the MYD variety employs a multifaceted defence mechanism that includes improved pathogen recognition (through R-genes), activation of immune signalling (MAPKs, WRKYs, and hormonal pathways), strengthening of structural barriers (cell wall biosynthesis), and efficient resource allocation (downregulation of sugar and flavonoid biosynthesis). The incorporation of transporter and detoxifying genes enhances MYD's capacity to respond swiftly and efficiently to RPW stress. This coordinated genetic response highlights the enhanced resistance of the MYD coconut variety and provides a significant basis for future coconut breeding initiatives focused on enhancing pest resilience.

Based on Table 4, in the present study, transcriptomic profiling identified key disease resistance genes upregulated in RPW-infested coconut palms across varieties, particularly putative disease resistance proteins RGA1, RGA3, and RGA4 from *Solanum bulbocastanum*, and RPS2 (Resistance to *Pseudomonas syringae* 2), annotated here as *DRL37_ARATH* from *Arabidopsis thaliana*. These genes are known to encode NB-LRR-type proteins involved in the recognition of pathogen-associated molecular patterns (PAMPs) and effector proteins. RGA proteins contain conserved NB-ARC and Rx N-terminal domains responsible for nucleotide binding and immune activation, while RPS2 is part of the well-characterized plant immune receptor family that mediates effector-triggered immunity (ETI), particularly in response to bacterial pathogens.

Table 4

Log2fold Change in Disease Resistance DEGs across Coconut Varieties. The different types of putative disease resistance gene (RGA) and ribosomal protein S2 (RPS2) show much higher level of expression in the resistant variety (MYD) compared to the susceptible varieties (Malayan Tall and Pandan).

Gene Name	Malayan Tall	MYD	Pandan
RPS2_ARATH	-	12.05	-
RGA1_SOLBU	1.21	3.84	3.38
RGA3_SOLBU	-	2.91	2.43
RGA3_SOLBU	-	2.54	-
RGA3_SOLBU	-	2.52	-
RGA3_SOLBU	-	2.46	-
RGA3_SOLBU	0.95	2.15	-
RGA1_SOLBU	1.32	2.14	-
RGA3_SOLBU	-	2.03	-
RGA1_SOLBU	-	1.99	-
RGA3_SOLBU	0.95	1.87	-
RGA4_SOLBU	-	1.65	-
RGA3_SOLBU	-	1.62	-
RGA3_SOLBU	0.78	1.54	-
RGA1_SOLBU	-	1.53	-
DRL13_ARATH	-	1.41	-
RGA3_SOLBU	0.65	0.96	1.63

Expression analysis revealed significant upregulation of RGA3 and RPS2 (DRL37_ARATH) in the MYD variety. Specifically, multiple isoforms of RGA3 exhibited high log2 fold changes in MYD (ranging from ~ 1.5 to ~ 2.9), indicating strong transcriptional activation of defense pathways. RGA1 was also upregulated across all varieties, but with notably higher expression in MYD. In contrast, RPS2 was exclusively upregulated in MYD (log2 fold change ≈ 12.05), with no detectable expression in Pandan or MT. This dramatic differential suggests that RPS2 may be a critical marker of MYD's heightened immunity against pathogens.

As shown in Fig. 9, the MYD variety exhibits the highest upregulation of DEGs across all transcription factor families, particularly in the MYB family. This suggests that MYD might have a stronger

transcriptional response in defense-related pathways compared to MT and Pandan.

The findings of this investigation indicate that the defence-related transcription factors were both upregulated and downregulated across all varieties, with the MYD variety demonstrating the number of upregulated genes in comparison to the Pandan and MT varieties. This encompasses NAC transcription factors such as NAC56, NAC-domain-containing proteins NAC22, NAC58, NAC68, NAC100 and NAC73 which are significant in enhancing stress tolerance and activating defense pathways (39). The expression levels of MYB transcription factors, including MYB30_ORYSJ and JAMYB_ORYSJ, were observed to increase, while MYB20, MYB44, and MYB60 demonstrated a decrease. This differential expression plays a crucial role in the regulation of defence gene expression (40). The expression levels of WRKY family transcription factors, including WRKY24, WRKY76, and WRKY55, were notably elevated in MYD, suggesting their involvement in facilitating immune responses in the context of RPW infestation (41). Alongside, the expression levels of ERF transcription factors, specifically ERF17, ERF071, ERF018, and ERF3, were found to be elevated, whereas ERF023 and ERF5 demonstrated reduced expression within the MYD integrated key stress signalling pathways, thereby enhancing defence mechanisms (42). The results highlight the robust defence response exhibited by MYD in relation to other varieties.

There was a notable increase in the expression of *Man2_Arath* and *RCA2_lartr* across

all three coconut varieties. Conversely, *Xth8_arath, Flz13_arath, Exol2_arath, and Anxd1_arath* exhibited a consistent and significant decrease in expression. This suggests a common transcriptional response characterized by the activation of basal defence genes, alongside the repression of cell wall remodelling, oxidative stress response, and hormone-regulated growth processes. In the context of RPW infestation, *Hsop2_arath, Acet1_orysj, and Dre2b_orysj* exhibited the highest levels of expression in Pandan, with MT following, and MYD showing the least expression. Additionally, *Crt1_arath and Syt4_arath* were also notably expressed in both Pandan and MT. This pattern suggests that the vulnerable varieties depend on the transcriptional activation of chaperone and membrane-associated stress response genes to uphold cellular homeostasis and structural integrity when robust resistance mechanisms are lacking.

RT-qPCR statistical analysis

RT-qPCR was conducted to validate the expression of selected genes as an independent assessment of RNA-seq data. It was demonstrated that the expression profile based on the up regulated expression of the selected genes in the three varieties as analyzed by RT-qPCR was coherent with the expression pattern obtained from RNA-seq data. There was no gene in the table exhibiting an expression pattern contradictory between both assessments. Additionally, 5 out of 6 genes tested (G245724, G328289, G35839, G358391, G359637 and G2812948) demonstrated that the infested MYD expression level was significantly different from the infested Pandan and infested MT as shown in Fig. 10. The substantial error bar indicates inherent biological variability among field-grown palms, rather than technical discrepancies. Environmental disparities, genetic diversity, and fluctuating pest infestation rates frequently amplify variance in biological replicates. This variability is characteristic of field-based plant defense studies and represents genuine biological diversity rather than measurement error.

Comparative analysis on SNP Variants

Single-nucleotide polymorphisms (SNPs) were identified within the promoter regions of the 17 differentially expressed disease-resistance genes. These genes include *RGA3* and *RPS2*, that encode NB-ARC domain–containing resistance proteins that play crucial roles in early pathogen recognition. The selected genes were previously shown to be highly expressed in the resistant MYD variety and downregulated in the susceptible Pandan and MT varieties. The identified SNPs were distributed across 8 of the 16 coconut chromosomes (Fig. 11).

Comparative SNP analysis among the three coconut variety pairs identified distinct genetic variation patterns between resistant and susceptible genotypes. Group 1 (MYD vs. Pandan) exhibited the highest polymorphism, with 846 SNPs across promoter regions of disease-resistance genes, indicating strong genetic divergence. Group 2 (MYD vs. MT) showed moderate variation with 684 SNPs, while Group 3 (Pandan vs. MT) had the fewest (368 SNPs), suggesting greater genetic similarity between the two susceptible varieties. The SNP distribution across the three pairwise comparisons is summarized in Table 5.

Table 5

The chromosome-wise distribution of SNP variants identified in pairwise comparisons between three coconut variety groups: Group 1 (MYD vs. Pandan), Group 2 (MYD vs. MT), and Group 3 (Pandan vs. MT). For each chromosome, the table includes the chromosome length, the number of variants detected in each group, and the total number of variants across all chromosomes for each group.

Chromosome	Length (bp)	Group 1	Group 2	Group 3
GWHBEBU00000003	186,073,739	213	187	80
GWHBEBU00000004	180,782,608	119	122	17
GWHBEBU00000005	175,769,743	70	79	15
GWHBEBU00000007	173,889,360	73	83	10
GWHBEBU00000010	151,372,088	1	13	14
GWHBEBU00000011	140,948,024	243	87	184
GWHBEBU00000014	91,061,363	60	58	14
GWHBEBU00000016	82,661,309	67	55	34
Total	**1,182,558,234**	**846**	**684**	**368**

Venn diagram analysis (Fig. 12) of the three pairwise comparisons Group 1 (MYD vs. Pandan), Group 2 (MYD vs. MT), and Group 3 (Pandan vs. MT) revealed substantial overlap in promoter-region SNPs among the groups. Groups 1 and 2 shared the highest overlap, with 575 common SNPs, indicating similar genetic variation patterns between MYD and both susceptible varieties. This suggests that MYD

may share conserved regulatory variants influencing disease resistance. No unique SNPs were detected in any single group, implying that all identified variants were shared with at least one other comparison.

Group 1 (MYD vs. Pandan) was selected for promoter motif analysis due to its highest SNP count and strongest overlap with other comparisons, indicating extensive genetic variation in regulatory regions. This group provided the best framework for identifying promoter motifs potentially linked to resistance mechanisms. Chromosomal distribution of SNP genotypes (Fig. 13) showed that most variants occurred in the susceptible Pandan variety, suggesting altered regulatory sequences associated with *Rhynchophorus ferrugineus* susceptibility. In contrast, the resistant MYD variety predominantly exhibited homozygous reference genotypes (0/0), reflecting a more stable promoter architecture and genomic consistency.

Statistical Analysis of SNP Variants in MYD and Pandan variety

FDR was applied to associate SNP variants with resistance or susceptibility to *Rhynchophorus ferrugineus*. Among 839 SNPs distinguishing the resistant MYD and susceptible Pandan varieties, 70 variants exhibited significant associations ($p < 0.05$) with the phenotypic classification, indicating their potential involvement in RPW resistance mechanisms.

The 70 SNPs significantly associated with RPW resistance were subjected to False Discovery Rate (FDR) correction to minimize Type I errors from multiple testing. Following adjustment, 49 variants with FDR-corrected p-values < 0.05 were retained as strong candidates for functional analysis and promoter motif annotation. Most significant SNPs occurred in the susceptible Pandan variety, whereas the resistant MYD exhibited minimal variation, predominantly homozygous reference genotypes (0/0). This pattern suggests that genetic variation contributing to RPW susceptibility is concentrated in regulatory promoter regions of the susceptible genotype, while MYD maintains greater genetic stability and potential resistance-associated conservation.

Significant SNP Variant in the promoter motif

Among the 49 SNPs significantly linked to susceptibility, 4 SNP variants were found to be significant above the threshold and only 3 variants were identified within the promoter motif region of gene g76386, highlighting the specific influence of these variants in the gene's regulatory regions as shown in Fig. 14.

Significant SNPs were located within key promoter motifs, including TATA-box, CAAT-box, and MYB elements (Table 6). Among the 17 analysed genes, only *g76386* contained SNPs within its promoter region, suggesting its regulatory role in coconut susceptibility to *Rhynchophorus ferrugineus*. These variants likely influence transcriptional activity through motif disruption. Three SNPs within these motifs were identified as potential gene-based markers for RPW susceptibility in coconut germplasm. This table highlights motifs identified in this sequence of promoter region along with the associated variants found in these regions. The motifs include TATA, CAAT-box and MYB motif.

Table 6
Motifs and Variants Identified in the Promoter Region

Motif SNP Position	Motif sequence in reference genome
TATA 62717576	TTCAGGACTTAGAGCCAT/CATAAAATATAACTTAAAAGAG
CAAT-box 62717891	TGTATTTGAAATACCATCAA/TATTAATATTTTTCTTGTTAAG
MYB 62718576	ATACCTGGAAGGAACT**G/C**TAACCATGGTTAAAAAGGAG

Discussion

The main findings of this study provide insights into the differential response of three varieties of mature coconut palm (Pandan, MT, and MYD) grown in Malaysia to RPW, the invasive insect pest. All the palms were collected from the same field site, minimizing the environmental variability. This setting allows us to capture the natural infestation of RPW in the coconut field, which makes this study different from other molecular studies that have been carried out in the past (43, 44). The field phenotypic data aligned with the molecular evidence to show MYD as the resistant variety while Pandan and MT as the susceptible varieties.

RPW has specific preferences in its attack points based on coconut variety, which is influenced by variations in trunk structure, plant height, and environmental exposure. In MT, the RPW was predominantly found to be entering through the base of the trunk, likely exploiting pre-existing entry points left by rhinoceros beetles (*Oryctes rhinoceros*) as a secondary infestation route, similar to previous observation (45). In contrast, in Pandan, RPW infestation occurred primarily through the crown region at the top of the tree, suggesting a more direct and aggressive mode of entry as reported in the previous study by (45). Despite these differences in the initial site of attack, both susceptible varieties eventually displayed similar characteristics of tissue damage, including wilting, the presence of tunnels or holes in the trunk, leaf discoloration, the detection of larvae or pupae, chewed cabbage, and death of the apical shoot as the final stage of infestation.

The transcriptional responses to RPW infestation are distinct among the three coconut varieties, as evidenced by their GO enrichment profiles. The GO data clearly demonstrate a significant divergence between the resistant (MYD) and susceptible (MT and Pandan) genotypes, despite a few shared baseline response pathways. Across all three varieties, there is a common enrichment of terms related to carbohydrate metabolism, cell wall structure, and primary metabolic processes, indicating that basal responses to pest attacks, such as reinforcement of the cell wall and adjustment of energy metabolism,

are enriched in all genotypes (46). GO terms like "cell wall," "cytoplasmic part," and "external encapsulating structure" suggest an attempt by each variety to maintain structural integrity during biotic stress (47). This shared profile reflects a generalized, evolutionarily conserved response to insect attack but does not in itself determine resistance.

Interestingly, genes like *Man2_arath* and *Rca2_lartr* were significantly upregulated across all three varieties, indicating their potential involvement in basal or induced defense mechanisms. The *Man2_arath* encodes the β-mannanase enzyme, which facilitates the hydrolysis of (1→4)-β-D-mannosidic linkages found in mannans, galactomannans, and glucomannans in plant cell walls (48). The increased activity of β-mannanase may play a role in the localized softening of cell walls, enabling the liberation of oligosaccharide fragments that function as damage-associated molecular patterns (DAMPs) (49). DAMPs can initiate subsequent defence signaling pathways, including the JA pathway, which is often linked to resistance against herbivores (50). *Xth8_arath, Flz13_arath, Exol2_arath*, and *Anxd1_arath* were downregulated across all three coconut varieties, suggesting RPW infestation may suppress cell wall remodelling, oxidative stress defence, and hormone-regulated growth. Suppression of *Xth8_arath*, an enzyme involved in xyloglucan metabolism and cell wall loosening (51) could possibly restrict tissue softening and insect penetration. Under pest pressure, suppression of *Flz13_arath*, a *SnRK1*-interacting protein, may indicate a change away from energy homeostasis and signalling integration (52). Downregulation of brassinosteroid-associated *Exol2_arath* and stress-related peroxidase *Anxd1_arath* suggests decreased growth signalling and ROS-scavenging (53). Altogether, the induced downregulated expression of the above-mentioned genes in all three varieties suggests altered cell wall modification and defense-related processes affecting structural integrity and stress recovery following RPW attack.

Several putative disease resistance genes *RGA3_ SOLBU* and *RPS2_ARATH (DRL37_ARATH)*, that encode NBC-ARC proteins and NBC-LRR protein, respectively, exhibited significant elevated expression levels in MYD in comparison to Pandan and MT. The regulation of NB-LRR proteins is mediated by the NB-ARC domain. NBS-LRR proteins belong to multigene families and play a crucial role in conferring resistance against a range of pathogens (54). The NB-ARC domain functions as a molecular switch that modulates immune activation by transitioning between an inactive state associated with Adenosine Diphosphate (ADP) and an active state associated with Adenosine Triphosphate (ATP). NB-LRR proteins utilize their LRR (*Leucine-rich repeat*) domain to detect effectors resulting from infestation and plant cell damage, thereby regulating NB-ARC activity (55).

The identification of DEGs corresponding to key disease resistance genes such as RPS2 further supports MYD enhanced immune capacity against RPW infestation, especially under higher weevil density (Population C), indicating their role in active defense (43). *RPS2_ARATH gene* that encodes the disease resistance protein RPS2 was initially characterised in *Arabidopsis thaliana* for its function in providing resistance to *Pseudomonas syringae*. The present dataset indicates that this gene was solely expressed and highly expressed in the MYD variety and not in the other two varieties. This gene is essential in effector-triggered immunity, indicating that *RPS2* could have a more extensive function in the

response to biotic stress, potentially encompassing insect herbivory. In alignment with this hypothesis, an independent transcriptomic investigation conducted on coconut revealed an upregulation of *RPS2* in response to RPW compared to healthy controls (8). The collective findings indicate that *RPS2_ARATH* may function as a conserved resistance gene, playing a crucial role in the early recognition and signalling processes against various biotic threats, such as RPW.

Notably enhanced expression of different families of transcription factors was observed in MYD with much lower expression or non-induced expression in the susceptible varieties. The findings indicate a notable increase in the expression levels of *WRKY24, WRKY76*, and *WRKY55* in the MYD coconut variety only. WRKYs play dual roles in regulating plant stress resistance and growth (41). Expression levels of *ERF17, ERF018, ERF114* and *ERF3* were elevated in MYD, contributing to enhanced immune responses. ERFs collaborate with GRAS transcription factors to annotate plant adaptation to stress and tissue repair, underscoring their essential function in plant resilience (56). Consistently, upregulated expression of gene belonging to GRAS transcription factor (*NRPB3_ARATH* and *PGLR2_PLAA*) was also observed in MYD but not in the other two susceptible varieties. NAC transcription factors are significant in regulating plant defense mechanisms through their interactions with phytohormones such as salicylic acid (SA), abscisic acid (ABA), JA, and ethylene (ET). The activation of the defense genes and hypersensitive responses concurrently influence cell division (57, 58). In a comparable way, the downregulation of *NAC68 and NAC100* MYD may promote growth, whereas the upregulation of *NAC56, NAC22, and NAC58* has the potential to improve stress tolerance (57). MYB transcription factors play a crucial role in regulating stress responses, metabolic processes, and tissue development (59). Their impact on defense mechanisms can be seen through structural alterations and the synthesis of protective compounds (60). MYD exhibited an elevated expression of the *MYB30_ORYSJ* and *JAMYB_ORYSJ* genes, contributing to the enhancement of defense mechanisms. Conversely, the expression levels of *MYB20, MYB44*, and *MYB60* were found to be decreased, which has implications for signaling pathways (31).

Mitogen-activated protein kinase (MAPK) cascade facilitates the transition from pathogen recognition to the activation of defense mechanisms upon the detection of pathogens (61). Receptor-like cytoplasmic kinases (RLCKs) initiate the activation of MAPKKKs, subsequently leading to the activation of MAPKs such as MPK3/6 or MPK4 (62). MAPK is a crucial role in the regulation of hormone signaling, the production of reactive oxygen species (ROS), the activation of defense-related genes, and the fortification of the cell wall. Recent findings indicate the existence of two signaling pathways associated with MAPK that are pertinent to insect resistance (63, 64). The MYD coconut variety exhibited a significant increase in the expression of *MAPKKK3 (MAPK3_ARATH)* and *TMK1*, which lesser upregulated expression in both Pandan and MT varieties. The MAP3K14-MKK3-MPK1/2/7/14 pathway, as documented in the literature, is known to be dependent on JA and is significant in the response to insect feeding (65), thereby reinforcing our findings.

MYD exhibits a significant downregulation of genes that are involved in the metabolism of polysaccharides and glucans, both of which are essential for the fortification of the cell wall, a physical barrier that can directly impede the penetration of insect larvae (66). Downregulation of XTH gene (

XTH25, XTH1 and *XTH8*), which encodes XTH enzymes that modify xyloglucan, would enhance cell wall flexibility (67, 68). Whereas, CAD genes play a crucial role in the formation of structural barriers and the regulation of SA-dependent pathways involved in lignin biosynthesis, contributing to resistance mechanisms (28, 28). The significance of *CADH_POPDE* in providing protection against pathogens has been highlighted in recent research (69) and this gene is downregulated in MYD. The present investigation highlights that cell wall is among gene ontology category enriched in both MYD and pandan. Interestingly, enrichment is higher in pandan potentially due to the greater extent of RPW attack. The greater degree of pathogen attack has been correlated with increased downregulation of key structural and defense-related genes, suggesting that intense biotic stress may suppress critical protective pathways in plants (70). MYD's capacity for rapid protein synthesis and intracellular reorganization, which are essential for conducting swift defense actions, is indicated by the additional enrichment of ribosomal structural constituents and cytoskeletal elements (71) .

The management of plant responses to stress induced by living organisms involves the utilization of hormonal signaling pathways for enhancement of resistance to pathogens. Ethylene signalling involves receptors located on the endoplasmic reticulum membrane. In MYD, the ethylene receptor *ETR2* and the transcription factor *ERF071* exhibited elevated expression levels, suggesting their potential involvement in the activation of defense mechanisms. Ethylene plays a crucial role in the stabilization of *ERF114*, a transcription factor that plays an important role in PevD1-induced disease resistance in *Arabidopsis thaliana* (72) by regulating the phenylpropanoid pathway. Higher expression of *ERF114* in the resistant variety, MYD, suggesting that ERF114 contributes to the enhancement of disease resistance compared to Pandan and MT. *ERF3*, found to be elevated in MYD, has been recognized in rice (*Oryza sativa*) as a gene that enhances the expression of trypsin proteinase inhibitors and plays a role in mediating resistance against *Chilo suppressalis* caterpillars (Lu et al., 2011). The elevation of the ACCO_MUSAC gene in MYD indicates a rise in ethylene production, highlighting its significance in stress response mechanisms. JA collaborates with SA, ET, and ABA to enhance stress adaptation through the initiation of systemic resistance (73), (74). JAMYB_ORYSJ exhibits elevated expression levels in MYD, underscoring its significance in defense mechanisms mediated by JA (75). The downregulation of the CHI gene in MYD results in an enhanced JA biosynthesis pathway, subsequently altering the defense responses (81), (82).

Enrichment in steroid metabolic and biosynthetic processes further implies the activation of hormone signalling, potentially through brassinosteroids (BRs) or related phytohormones, which are known to fine-tune immune responses (73). Brassinosteroids play a crucial role in the equilibrium between growth and defense mechanisms (74). The infestation of RPW results in a decrease in the expression of the BZR1 gene, consequently leading to a reduction in BRs, as reported by (75, 76). The observed downregulation of this gene indicates a potential mechanism for energy conservation during defense responses (77). The downregulation of BRs in MYD also indicates a possible alteration in hormone signaling that prioritizes plant defense mechanisms; reduced levels of BRs may hence enhance JA- and SA-mediated defense responses (78, 79).

ABC transporters employ ATP hydrolysis to transport many compounds, including secondary metabolites like terpenoids, alkaloids, and phenolics, which serve as essential chemical defences against diseases and herbivorous insects (80) where excessive amounts could be phytotoxic (81). Particularly, several ABC transporters, including *NtABCG5* (also referred to as *NtPDR5)* increased in reaction to insect herbivory (82). Hence, the upregulation of the ABC transporter gene in MYD aligns with the previous studies to enhance the plant defense system with transporting out the toxin due to pest attack. Apart from that, despite being synthesized intracellularly, BRs perform their function at the cell surface, necessitating an export route for their action. Recent investigations have identified the ATP-binding cassette (ABC) transporter *ABCB19_ARATH* gene, previously identified as a crucial mediator of BR export. BRs were demonstrated to activate *ABCB19*'s ATPase activity and be translocated via this pathway (83). In our investigation, the observed overexpression of ABC transporters in response to insect infestation presumably enhances the export of BRs, hence elucidating the simultaneous downregulation of intracellular BR levels.

The present study also revealed an increased number of genes that respond indirectly to stress. This encompasses genes responsible for encoding heat shock proteins (HSPs), with a particular emphasis on *HSP82*, which play a vital role in preserving protein stability and enhancing immune responses (84, 85). The involvement of these entities in both PTI and ETI responses is facilitated through the recognition of PAMPs and pathogen effector molecules (86, 87). BAG proteins play a crucial role in the regulation of stress signals and the facilitation of chaperone functions. The increase in expression levels of *BAG5_ARATH* and *DNJ1_CAEEL* in MYD indicate a potential for enhanced stress adaptation, as evidenced by the findings [86] as BAG proteins are conserved regulators of apoptosis and stress responses seen in mammals, plants, and yeasts. The *TAAC* gene is crucial for the 3'-Phosphoadenosine 5'-phosphosulfate (PAPS) transporter and is integral to the process of sulfation in response to stress (77). The metabolism of sucrose plays a crucial role in defense mechanisms, as a reduction in *SUS1_TULGE* may limit sugar availability for pathogens (30, 88, 89). Both TAAC and *SUS1_TULGE* were highly downregulated in MYD. The observed reduction in *GSTF12* and *GSTF3* observed in MYD indicates a change in the management of reactive oxygen species (90, 91) whereas the decline in *CTR1* is associated with elevated ethylene levels (31, 92).

The expression level of *Hsop2_arath, Acet1_orysj*, and *Dre2b_orysj* was notably highest in Pandan, followed by MT and much lower in MYD. The gene *Hsop2_arath* belonging to the HOP family encodes a co-chaperone protein that facilitates the functional interaction between HSP70 and HSP90 chaperones (93).The calcium-binding molecular chaperone *Crt1_arath* was highly expressed in in Pandan and MT indicating increased endoplasmic reticulum (ER) protein-folding activity and quality control under stress. *Crt1* plays significant roles in calcium homeostasis, protein folding, reproduction, and the responses to both abiotic and biotic stresses in *Arabidopsis thaliana*, *Oryza sativa* (rice), *Nicotiana tabacum* (tobacco), *Solanum lycopersicum* (tomato), *Zea mays* (maize) and *Triticum aestivum* (wheat) (94). Syt4_arath, a phloem-associated protein implicated in membrane fluidity and stress responses was highly expressed in both susceptible varieties. It is associated with membrane trafficking that promotes defence signalling or cellular repair and was reported to be involved in abiotic stress such as osmotic,

cold, and salinity stress in *Arabidopsis* thaliana (95). Altogether, the expression of these genes suggests that Pandan and MT showed parallel coordinated transcriptional response to regulate cellular stress and retain metabolic and structural functions, however the defense system is not strong enough to resist RPW attack resulting in the observed symptoms.

The different category of genes with showed altered expression in MYD including cell wall modification, hormonal signalling, disease resistance, ABC transporters and stress response genes indicate a coordinated and strong defence response contributing to resistance to RPW. The condition of the susceptible plants in the field (damage level 2) most probably led to the unaltered or much reduced change of expression of these genes in the susceptible coconut varieties, MT and Pandan. However, it cannot be ruled out these could be attributed to genotypic differences in their defence response mechanisms such as the presence of DNA mutation in the regulatory region that prevent the gene activation in response to the insect or elicitor secretion. Molecular responses to important coconut pests such as *Rhynchophorus ferrugineus* and *Oryctes rhinoceros* have uncovered defense-related genes associated with JA signalling and secondary metabolite biosynthesis (43, 96, 97). SSR and RAPD marker analyses for coconut mite (*Aceria guerreronis*) have revealed molecular marker combinations that account for up to 100% of resistance association, showing the efficacy of molecular techniques in early screening and breeding (98). Collectively, the previous studies along with this current transcriptomic data across different coconuts varieties are important contributions in comprehending resistance mechanisms facilitating marker-assisted selection and guided sustainable pest management in coconut.

This study identified genetic variations and potential gene-based markers associated with RPW infestation in three coconut varieties: Pandan, MYD and MT. Resequencing data identified 987 SNPs in the promoter region of 17 disease-resistance genes, highlighting distinct genetic differences between resistant and susceptible varieties. MYD exhibited greater genomic stability and resistance, while Pandan showed a higher frequency of promoter-region SNPs linked to susceptibility. High-throughput sequencing has revolutionized the discovery of SNP markers that underlie important agronomic traits such as stress tolerance, flowering, and fruit quality (95, 99). SNPs in both coding and non-coding regions can alter gene expression by affecting protein structure or transcriptional regulation (100). In this study, most functionally relevant SNPs were found in promoter regions suggesting a regulatory basis for RPW susceptibility in Pandan. SNPs have proven effective as reliable molecular markers to differentiate resistant and susceptible genotypes in plants (101, 102). Similar findings have been reported in other crops, such as nematode tolerance in sugar beetroot linked to *HsBvm-1* (103).

Identifying three SNPs within the *RGA3* promoter in the susceptible Pandan variety suggests potential disruption of transcription factor binding sites and reduced promoter activity. Since RGA3 encodes an NB-ARC domain–containing resistance protein involved in pathogen recognition and immune signaling, promoter alterations may downregulate defense gene expression, increasing RPW susceptibility. These variants represent promising regulatory markers for breeding and functional validation. The presence of promoter SNPs in this gene likely affects transcriptional activation, thereby modulating defence

responses. Regulatory SNPs (rSNPs) located in promoter motifs can alter transcription factor binding and, consequently, gene expression (104). The significant promoter variants identified in this study support this mechanism, revealing that changes in regulatory motifs can suppress gene expression in susceptible varieties. For instance, the absence of *RGA3* expression in Pandan, compared with its upregulation in MYD, may result from rSNPs affecting transcription factor binding efficiency. Similar non-coding SNPs affecting gene regulation have been reported in the *FLOWERING LOCUS C* (*FLC*) gene of *Arabidopsis thaliana*, influencing phenotypic adaptation (105). Three principal promoter motifs, namely the TATA-box, CAAT-box, and MYB binding sites, were identified as harbouring rSNPs in the *RGA3* promoter of the susceptible Pandan variety. Promoter motifs are essential cis-regulatory elements that mediate transcription initiation and transcription factor recruitment (106). Mutations within these motifs can significantly alter gene expression (107). The identified SNPs in Pandan may interfere with transcription factor binding, leading to reduced transcription of resistance genes during RPW attack.

The MYB transcription factor family plays a pivotal role in plant defence regulation. The R2R3-MYB proteins recognize conserved DNA motifs (e.g., TAACCA) and modulate transcription of stress-response genes (41, 108). In this study, a G/C polymorphism immediately upstream of the MYB motif in Pandan (variant GTAACCA) did not alter the motif itself but may influence local DNA conformation or binding affinity. Although the core motif remained intact, subtle positional variations may still influence the timing or strength of MYB-mediated transcriptional activation. The TATA-box, typically positioned 25–35 bp upstream of the transcription start site, serves as the core promoter element that recruits TATA-binding protein (TBP) for pre-initiation complex formation (109). A T→C substitution identified in Pandan (TATAAAAT → CATAAAAT) likely disrupts TBP binding. Even minor sequence alterations in the TATA-box can reduce transcription initiation efficiency, thereby limiting gene expression (110, 111). This mutation could partly explain the downregulation of *RGA3* in the susceptible variety under RPW infestation. Similarly, a SNP identified within the CAAT-box (CAAAT → CATAT) in Pandan may impair binding of CAAT-binding factors, essential for transcriptional activation (112, 113). Such mutations can disrupt transcription initiation, as observed in animal and plant systems (114, 115). In the *TNP1* gene of Sahiwal cattle, similar promoter SNPs affected transcription factor binding and altered gene expression, demonstrating how promoter polymorphisms can regulate key traits (115). A comparable mechanism may underlie the decreased resistance gene expression observed in Pandan.

A key observation is that several of the identified heterozygous (0/1) genotype, SNPs are located within or near promoter regulatory motifs, including the TATA-box, CAAT-box, and MYB-like transcription factor binding sites. Variants within these cis-regulatory elements are known to affect transcription initiation and transcription factor binding affinity (115). Even single nucleotide substitutions can modulate promoter performance by weakening motif integrity, thereby altering the expression of downstream genes. Thus, the heterozygous SNPs in the susceptible pandan may result in differential promoter activity between alleles one functioning normally and the other exhibiting reduced regulatory efficiency.

Heterozygous promoter SNPs have also been reported to contribute significantly to phenotypic diversity in plants, especially traits related to stress response and disease (116). In many crop species, such

polymorphisms can create dosage effects or incomplete dominance, leading to weakened transcriptional activation of key defence genes (117). In the context of pandan susceptibility, the presence of heterozygous SNPs within promoter motifs may reduce the overall regulatory robustness of the affected genes. Although the reference allele remains the same, the alternate allele may diminish binding by essential transcription factors such as MYB proteins, potentially impairing defence signalling pathways.

Overall, these findings reinforce that promoter-region SNPs play a pivotal role in determining gene expression patterns that define resistance or susceptibility in coconuts. Variations within cis-regulatory motifs such as the TATA-box, CAAT-box, and MYB-binding sites can significantly alter transcriptional dynamics. The resistant MYD variety, with fewer promoter SNPs and stable homozygous reference genotypes, likely maintains optimal transcriptional regulation of resistance genes. In contrast, Pandan's accumulation of promoter polymorphisms may weaken defence gene activation, leading to increased vulnerability to RPW infestation.

Conclusion

This is the first report on comparative transcriptomics on the response of resistant and susceptible coconut varieties to RPW infestation in the field. The initial phenotypic characterisation showed the different levels of susceptibility to RPW leading to the classification of MYD as the resistant while both Pandan and MT as the susceptible varieties. RNA sequencing revealed that the MYD variety exhibits a more robust molecular defence network, marked by the upregulation of several defence-related genes. Among them included seventeen candidate genes associated with disease resistance demonstrating markedly elevated expression levels in MYD variety in contrast to Pandan and MT varieties. The activation of multiple signalling pathways, with a particular emphasis on the MAPK cascade, essential for the transmission of stress signals and the modulation of immune responses was observed in MYD. The participation of ABC transporters and heat shock proteins indicates that MYD not only activates defence genes but also enhances cellular protective mechanisms to mitigate stress-induced damage. MYD also showed significantly stronger altered expression of genes associated with phytohormones, including JA and ET, which are recognised as essential regulators of plant immune responses. Key transcription factor families such as the NAC, WRKY, MYB, ERF and CAMTA that act as essential regulators of plant growth, development, and defence, integrating complex signalling networks to balance stress responses and growth showed stronger up or down-regulated expression in MYD compared to MT and Pandan. This research has also identified the genetic variation in the promoter region of the chosen 17 DEGs encoding disease resistance genes among the three coconut varieties studied. This study reinforces the discovery by identifying three significant SNP variants in the promoter of the *RGA3* disease resistance gene in the MYB-binding motif, TATA-box, and CAAT-box. This variant can alter the transcription factor binding site, affecting the affinity of the DNA binding protein and ultimately hindering the initiation and efficiency of gene transcription. The identified SNPs could serve as markers for breeding efforts aimed at improving resistance traits in coconut crops. Future studies will aim to

validate these findings by conducting functional analyses of the identified SNPs and exploring their potential roles in gene regulation and phenotypic expression.

Abbreviations

ABC
ATP-Binding Cassette
ABCB19_ARATH
Arabidopsis ABC transporter B19
ARC
APAF-1, R proteins, and CED-4 domain
BAG
Bcl-2-associated athanogene
bp
Base Pair
BR
Brassinosteroid
BRs
Brassinosteroids
BRI1
Brassinosteroid Insensitive 1
BZR1
Brassinazole Resistant 1
CAD
Cinnamyl Alcohol Dehydrogenase
CAMTA
Calmodulin-binding Transcription Activator
CC
Cellular Component
cDNA
Complementary DNA
CnEF-1α
Cocos nucifera Elongation Factor 1 alpha
CneIF-4γ
Cocos nucifera Eukaryotic Initiation Factor 4 gamma
CTR1
Constitutive Triple Response 1
DEG
Differentially Expressed Gene
DEGs

Differentially Expressed Genes
DNA
Deoxyribonucleic Acid
DNJ1_CAEEL
DnaJ homolog from Caenorhabditis elegans
DND1_CUCSA
Defense No Death 1 (*Cucumis sativus*)
DRL
Disease Resistance-Like
DRL37_ARATH
Disease Resistance-Like 37 (*Arabidopsis thaliana*)
DREB
Dehydration-Responsive Element-Binding
eEF1A
Eukaryotic Elongation Factor 1 Alpha
ERF
Ethylene Response Factor
ET
Ethylene
ETI
Effector-Triggered Immunity
FDR
False Discovery Rate
FMYDC
Malayan Yellow Dwarf Control
FMYDI
Malayan Yellow Dwarf Infested
FMTC
Malayan Tall Control
FMTI
Malayan Tall Infested
FPC
Pandan Control
FPI
Pandan Infested
FPKM
Fragments Per Kilobase of transcript per Million mapped reads
GO
Gene Ontology
GRAS

GAI, RGA, and SCR (transcription factor family)
GST
Glutathione S-Transferase
GSTF3
Glutathione S-Transferase F3
GSTF12
Glutathione S-Transferase F12
GSTs
Glutathione S-Transferases
HOP
Hsp70-Hsp90 Organizing Protein
HR
Hypersensitive Response
HSP
Heat Shock Protein
HSP82
Heat Shock Protein 82
Hsop2_arath
Heat Shock Protein 2 (Arabidopsis thaliana)
JA
Jasmonic Acid
LiCl
Lithium Chloride
MAPK
Mitogen-Activated Protein Kinase
MAPK3_ARATH
Mitogen-Activated Protein Kinase 3 (Arabidopsis thaliana)
MAPKs
Mitogen-Activated Protein Kinases
MF
Molecular Function
mRNA
Messenger RNA
MQ
Mapping Quality
MT
Malayan Tall
MYB
Myeloblastosis Transcription Factor
MYD

Malayan Yellow Dwarf
NAC
NAM, ATAF, and CUC transcription factor family
NB-LRR
Nucleotide-Binding Leucine-Rich Repeat
NBS-LRR
Nucleotide-Binding Site Leucine-Rich Repeat
NtABCG5
Nicotiana tabacum ABCG5
NtPDR5
Nicotiana tabacum Pleiotropic Drug Resistance 5
PAMP
Pathogen-Associated Molecular Pattern
PAPS
3'-Phosphoadenosine 5'-Phosphosulfate
PCR
Polymerase Chain Reaction
PTI
PAMP-Triggered Immunity
Q20
Quality Score 20 (Base-calling accuracy)
qPCR
Quantitative Polymerase Chain Reaction
RNA
Ribonucleic Acid
RNA-seq
RNA Sequencing
RGA
Resistance Gene Analog
RGA1, RGA3, RGA4
Resistance Gene Analogs 1, 3, and 4
RGA3_SOLBU
Resistance Gene Analog 3 (*Solanum bulbocastanum)*
RIN
RNA Integrity Number
RPS2
Resistance to *Pseudomonas syringae 2*
ROS
Reactive Oxygen Species
RPW

Red Palm Weevil
SA
Salicylic Acid
SEM
Standard Error of Mean
SNP
Single Nucleotide Polymorphism
SNPs
Single Nucleotide Polymorphisms
SUS1_TULGE
Sucrose Synthase 1 (*Tulipa gesneriana)*
TAAC
Thylakoid ADP/ATP Carrier
TATA-box
Core promoter sequence
TOR
Target of Rapamycin
UGT71
UDP-glucosyltransferase 71
UAV
Unmanned Aerial Vehicle
VCF
Variant Call Format
WRKY
WRKY Transcription Factor Family
XTH
Xyloglucan Endotransglycosylase/ Hydrolase

Declarations

Ethics declarations

Ethics approval and consent to participate

Not applicable.

Consent for publication

Not applicable.

Competing interests

The authors declare that they have no competing interests.

Publisher's Note

Springer Nature remains neutral with regard to jurisdictional claims in published maps and institutional affiliations.

Availability of data and materials

The RNA sequencing datasets generated and/or analysed during the current study have been deposited in the NCBI BioProject and BioSample databases and being processed. The BioProject ID is PRJNA1375459 and can be accessed at https://www.ncbi.nlm.nih.gov/bioproject/1375459.

The BioSample accessions for the sequenced samples are:

Pandan variety: SAMN53685843, SAMN53685844, SAMN53685845, SAMN53685846, SAMN53685847, SAMN53685848

Malayan Tall variety: SAMN53685849, SAMN53685850, SAMN53685851, SAMN53685852, SAMN53685853, SAMN53685854

Malayan Yellow Dwarf variety: SAMN53685855, SAMN53685856, SAMN53685857, SAMN53685858, SAMN53685859, SAMN53685860

These datasets are publicly available for download and reuse under the standard NCBI repository guidelines.

Funding

This work was supported/funded by Ministry of Higher Education under the Long-Term Research Grant Scheme (LRGS) LRGS/1/2020/UPM/01/2.

Authors contribution

UM designed and carried out the experimental work, data analysis, and interpretation. SNAA supervised the study, reviewed and edited the manuscript. NM contributed to technical validation and data acquisition. All authors read and approved the final version of the submitted manuscript.

Correspondence to:

Siti Nor Akmar Abdullah

Institute of Plantation Studies, Universiti Putra Malaysia, 43400 UPM, Serdang, Selangor, Malaysia

Email: snaa@upm.edu.my

Acknowledgement

This work was supported/funded by Ministry of Higher Education under the Long-Term Research Grant Scheme (LRGS) LRGS/1/2020/UPM/01/2. We are also thankful to Department of Agriculture Malaysia for assisting with field screening and sampling

References

1. Niral V, Jerard BA. Botany, origin and genetic resources of coconut. The Coconut Palm (Cocos nucifera L) - Research and Development Perspectives. Springer Singapore; 2019. pp. 57–111.
2. Arumugam T, Hatta MAM. Improving Coconut Using Modern Breeding Technologies: Challenges and Opportunities. Plants (Basel). 2022;11(24):3414.
3. Arhin L, Abdullah S, nor A, Jaafar JN, Izan Ramlee S. Conventional and modern breeding technologies for improving dwarf coconut cultivars: A review. J Hortic Sci Biotechnol 2023 Sept 3;98(5):551–62.
4. Delalieux S, Hardy T, Ferry M, Gomez S, Kooistra L, Culman M, et al. Red Palm Weevil Detection in Date Palm Using Temporal UAV Imagery. Remote Sens. 2023;15(5):1380.
5. Giblin-Davis R, Faleiro JR, Jaques J, Pena J, Vidyasagar P. In. Biology and Management of the Red Palm Weevil, Rhynchophorus ferrugineus. 2013. p. 33.
6. Azmi W, Chong Jlian, Ahamad Zakeri H, Yusuf N, Wan Omar WB, Wai Y, et al. The Red Palm Weevil, Rhynchophorus ferrugineus: Current Issues and Challenges in Malaysia. Oil Palm Bull. 2017;74:17–24.
7. Abraham VA, Faleiro JR, Radhakrishnan Nair CP, Nair SS. Present Management Technologies For Red Palm Weevil, Rhynchophorus Ferrugineus Oliver (Coleopteran: Curculionidae) In Palms And Future Thrusts. 2002 Dec [cited 2025 Jan 24]; Available from: http://hdl.handle.net/123456789/5629
8. Soroker V, Blumberg D, Haberman A, Hamburger-Rishard M, Reneh S, Talebaev S, et al. Current status of red palm weevil infestation in date palm plantations in Israel. Phytoparasitica. 2005;33:97–106.
9. Boulila W, Alzahem A, Koubaa A, Benjdira B, Ammar A. Early detection of red palm weevil infestations using deep learning classification of acoustic signals. Computers Electron Agric 2023 Sept 1;212:108154.
10. Senafi NS, Mohamed NZ, Azmi WA. Population Abundance of Red Palm Weevil, Rhynchophorus ferrugineus (Coleoptera: Dryophthoridae) in Rhu Tapai Coconut Plantation. Universiti Malaysia Terengganu J Undergrad Res. 2020;2(1):71–6.
11. Hasim N, Yusuf N, HYDROGEN, PEROXIDE, LIPID PEROXIDATION AND TOTAL ION LEAKAGE IN, COCONUT CULTIVAR. Malays Appl Biol. 2017;46:221–8.
12. War AR, Paulraj MG, Ahmad T, Buhroo AA, Hussain B, Ignacimuthu S, et al. Mechanisms of plant defense against insect herbivores. Plant Signal Behav. 2012;7(10):1306–20.

13. Jones JDG, Dangl JL. The plant immune system. Nature. 2006;444(7117):323–9.
14. Chen CY, Mao YB. Research advances in plant–insect molecular interaction. F1000Res. 2020;9:F1000 Faculty Rev-198.
15. Andersen EJ, Ali S, Byamukama E, Yen Y, Nepal MP. Disease Resistance Mechanisms in Plants. Genes. 2018 July;9(7):339.
16. Chaudhary R, Atamian H. Resistance-Gene-Mediated Defense Responses against Biotic Stresses in the Crop Model Plant Tomato. J Plant Pathol Microbiol. 2017;08.
17. Rajesh MK, Gangurde SS, Pandey MK, Niral V, Sudha R, Jerard BA et al. Insights on Genetic Diversity, Population Structure, and Linkage Disequilibrium in Globally Diverse Coconut Accessions Using Genotyping-by-Sequencing. OMICS: A Journal of Integrative Biology. 2021;25(12):796–809.
18. Mekso M, Feyissa T. RNA-Seq as an Effective Tool for Modern Transcriptomics, A Review-based Study. J Appl Res Plant Sci 2022 July 30;3:236–41.
19. Nejat N, Cahill DM, Vadamalai G, Ziemann M, Rookes J, Naderali N. Transcriptomics-based analysis using RNA-Seq of the coconut (Cocos nucifera) leaf in response to yellow decline phytoplasma infection. Mol Genet Genomics. 2015;290(5):1899–910.
20. Gangaraj KP, Rajesh MK. Dataset of dual RNA-sequencing of *Phytophthora palmivora* infecting coconut (*Cocos nucifera* L.). Data in Brief. 2020 June 1;30:105455.
21. Song B, Ning W, Wei D, Jiang M, Zhu K, Wang X, et al. Plant genome resequencing and population genomics: Current status and future prospects. Mol Plant. 2023;16(8):1252–68.
22. Gage JL, Mali S, McLoughlin F, Khaipho-Burch M, Monier B, Bailey-Serres J et al. Variation in upstream open reading frames contributes to allelic diversity in maize protein abundance. Proceedings of the National Academy of Sciences. 2022;119(14):e2112516119.
23. Wang S, Xiao Y, Zhou ZW, Yuan J, Guo H, Yang Z, et al. High-quality reference genome sequences of two coconut cultivars provide insights into evolution of monocot chromosomes and differentiation of fiber content and plant height. Genome Biol. 2021;22(1):304.
24. Rajesh MK, Budhwar R, Shukla R, Oraon PK, Goel S, Paul B, et al. Chromosome scale genome assembly and annotation of coconut cultivar Chowghat Green Dwarf. Sci Rep. 2024;14(1):28778.
25. Rachana KE, Rajesh MK. Selection and validation of reference genes for gene expression normalization in coconut (Cocos nucifera L.) under biotic stress and hormone stimuli. Plant Gene. 2019 Sept;19:100184.
26. Xu J, Zhang S. Mitogen-activated protein kinase cascades in signaling plant growth and development. Trends Plant Sci. 2015;20(1):56–64.
27. TRONCHET M, BALAGUÉ C, KROJ T. Cinnamyl alcohol dehydrogenases-C and D, key enzymes in lignin biosynthesis, play an essential role in disease resistance in Arabidopsis. Mol Plant Pathol. 2009;11(1):83–92.
28. Yokoyama R, Nishitani K. A comprehensive expression analysis of all members of a gene family encoding cell-wall enzymes allowed us to predict cis-regulatory regions involved in cell-wall

construction in specific organs of Arabidopsis. Plant Cell Physiol. 2001;42(10):1025–33.

29. Stein O, Granot D. An Overview of Sucrose Synthases in Plants. Front Plant Sci [Internet]. 2019 Feb 8 [cited 2025 Jan 5];10. Available from: https://www.frontiersin.org/journals/plant-science/articles/10.3389/fpls.2019.00095/full
30. Wang Q. Study on the expression regulation of the *CTR1* gene in the ethylene signaling pathway. Biochem Biophys Res Commun. 2024;739:150590.
31. Cao X, Wei Y, Shen B, Liu L, Mao J. Interaction of the Transcription Factors BES1/BZR1 in Plant Growth and Stress Response. Int J Mol Sci. 2024 June 21;25(13):6836.
32. Ngaki MN, Louie GV, Philippe RN, Manning G, Pojer F, Bowman ME, et al. Evolution of the Chalcone Isomerase Fold from Fatty Acid-Binding to Stereospecific Enzyme. Nature. 2012;485(7399):530–3.
33. Hu C, Yang J, Qi Z, Wu H, Wang B, Zou F et al. Heat shock proteins: Biological functions, pathological roles, and therapeutic opportunities. MedComm (2020). 2022;3(3):e161.
34. Mazari AMA, Zhang L, Ye ZW, Zhang J, Tew KD, Townsend DM. The Multifaceted Role of Glutathione S-Transferases in Health and Disease. Biomolecules. 2023;13(4):688.
35. Ren R, Yang X, Xu J, Zhang K, Zhang M, Liu G, et al. Genome-wide identification and analysis of promising GDSL-type lipases related to gummy stem blight resistance in watermelon (*Citrullus lanatus*). Sci Hort. 2021;289:110461.
36. Yazaki K. ABC transporters involved in the transport of plant secondary metabolites. FEBS Lett. 2006;580(4):1183–91.
37. Harjes S, Scheidig A, Bayer P. Expression, purification and crystallization of human 3'-phosphoadenosine-5'-phosphosulfate synthetase 1. Acta Crystallogr D Biol Crystallogr. 2004;60(Pt 2):350–2.
38. Nuruzzaman M, Sharoni AM, Kikuchi S. Roles of NAC transcription factors in the regulation of biotic and abiotic stress responses in plants. Front Microbiol 2013 Sept 3;4:248.
39. Geng P, Zhang S, Liu J, Zhao C, Wu J, Cao Y, et al. MYB20, MYB42, MYB43, and MYB85 Regulate Phenylalanine and Lignin Biosynthesis during Secondary Cell Wall Formation1[OPEN]. Plant Physiol. 2020;182(3):1272–83.
40. Wang X, Li J, Guo J, Qiao Q, Guo X, Ma Y. The WRKY transcription factor PlWRKY65 enhances the resistance of Paeonia lactiflora (herbaceous peony) to Alternaria tenuissima. Hortic Res. 2020;7(1):1–12.
41. Abiri R, Shaharuddin NA, Maziah M, Yusof ZNB, Atabaki N, Sahebi M, et al. Role of ethylene and the APETALA 2/ethylene response factor superfamily in rice under various abiotic and biotic stress conditions. Environ Exp Bot. 2017;134:33–44.
42. Liu L, Yan W, Liu B. Transcriptome sequencing of Cocos nucifera leaves in response to Rhynchophorus ferrugineus infestation. Frontiers in Genetics [Internet]. 2023 [cited 2023 Aug 11];14. Available from: https://www.frontiersin.org/articles/10.3389/fgene.2023.1115392

43. Liu L, Yan W, Liu B, Qin W. Molecular Insights into Red Palm Weevil Resistance Mechanisms of Coconut (Cocos nucifera) Leaves. Plants (Basel). 2024 July 12;13(14):1928.
44. Azmi W. A New Invasive Coconut Pest in Malaysia: the Red Palm Weevil (Curculionidae: Rhynchophorus ferrugineus). Planter. 2013;89:97–110.
45. Kerchev PI, Fenton B, Foyer CH, Hancock RD. Plant responses to insect herbivory: interactions between photosynthesis, reactive oxygen species and hormonal signalling pathways. Plant Cell Environ. 2012;35(2):441–53.
46. Bellincampi D, Cervone F, Lionetti V. Plant cell wall dynamics and wall-related susceptibility in plant–pathogen interactions. Front Plant Sci [Internet]. 2014 May 28 [cited 2025 July 4];5. Available from: https://www.frontiersin.org/journals/plant-science/articles/10.3389/fpls.2014.00228/full
47. de Petkowicz O, Reicher CL, Chanzy F, Taravel H, Vuong FR. Linear mannan in the endosperm of *Schizolobium amazonicum*. Carbohydr Polym. 2001;44(2):107–12.
48. Pontiggia D, Benedetti M, Costantini S, De Lorenzo G, Cervone F. Dampening the DAMPs: How Plants Maintain the Homeostasis of Cell Wall Molecular Patterns and Avoid Hyper-Immunity. Front Plant Sci. 2020;11:613259.
49. Quintana-Rodriguez E, Duran D, Heil M, camacho coronel X. Damage-associated molecular patterns (DAMPs) as future plant vaccines that protect crops from pests. Scientia Horticulturae 2018 July 14;237:207–20.
50. Divol F, Vilaine F, Thibivilliers S, Kusiak C, Sauge MH, Dinant S. Involvement of the xyloglucan endotransglycosylase/hydrolases encoded by celery XTH1 and Arabidopsis XTH33 in the phloem response to aphids. Plant Cell Environ. 2007;30(2):187–201.
51. Feng L, Li X, Zheng XA, Zheng Z, Liu QR, Liu C et al. SnRK1 and TOR: central regulators of autophagy in plant energy stress responses. aBIOTECH [Internet]. 2025 May 15 [cited 2025 July 15]; Available from: https://doi.org/10.1007/s42994-025-00218-3
52. Clouse SD, Langford M, McMorris TC. A brassinosteroid-insensitive mutant in Arabidopsis thaliana exhibits multiple defects in growth and development. Plant Physiol. 1996 July;111(3):671–8.
53. Jiang Y, Li Z, Li W, Cheng H, Zhao W, Li T, et al. Genome-Wide Analysis Revealed NBS-LRR Gene Candidates Associated with Bacterial Wilt Resistance in Eggplant (Solanum melongena L). Agronomy. 2023;13(10):2583.
54. Steele JFC, Hughes RK, Banfield MJ. Structural and biochemical studies of an NB-ARC domain from a plant NLR immune receptor. PLoS ONE. 2019;14(8):e0221226.
55. Neves C, Ribeiro B, Amaro R, Expósito J, Grimplet J, Fortes AM. Network of GRAS transcription factors in plant development, fruit ripening and stress responses. Hortic Res 2023 Sept 27;10(12):uhad220.
56. Bian Z, Gao H, Wang C. NAC Transcription Factors as Positive or Negative Regulators during Ongoing Battle between Pathogens and Our Food Crops. Int J Mol Sci. 2020;22(1):81.
57. Seo PJ, Kim MJ, Park JY, Kim SY, Jeon J, Lee YH, et al. Cold activation of a plasma membrane-tethered NAC transcription factor induces a pathogen resistance response in Arabidopsis. Plant J.

2010;61(4):661–71.

58. Mariyam S, Kumar V, Roychoudhury A, Ghodake GS, Muneer S, Duhan JS et al. Functional Diversification and Mechanistic Insights of MYB Transcription Factors in Mediating Plant Growth and Development, Secondary Metabolism, and Stress Responses. J Plant Growth Regul [Internet]. 2025 Jan 27 [cited 2025 Mar 14]; Available from: https://doi.org/10.1007/s00344-025-11622-w
59. Biswas D, Gain H, Mandal A. MYB transcription factor: A new weapon for biotic stress tolerance in plants. Plant Stress. 2023;10:100252.
60. Zhang M, Zhang S. Mitogen-activated protein kinase cascades in plant signaling. J Integr Plant Biol. 2022;64(2):301–41.
61. Bi G, Zhou Z, Wang W, Li L, Rao S, Wu Y et al. Receptor-Like Cytoplasmic Kinases Directly Link Diverse Pattern Recognition Receptors to the Activation of Mitogen-Activated Protein Kinase Cascades in Arabidopsis. The Plant Cell. 2018 July 1;30(7):1543–61.
62. Romero-Hernandez G, Martinez M. Plant Kinases in the Perception and Signaling Networks Associated With Arthropod Herbivory. Front Plant Sci [Internet]. 2022 May 4 [cited 2025 July 14];13. Available from: https://www.frontiersin.org/journals/plant-science/articles/10.3389/fpls.2022.824422/full
63. Romero-Hernandez G, Martinez M. Opposite roles of MAPKKK17 and MAPKKK21 against Tetranychus urticae in Arabidopsis. Front Plant Sci. 2022;13:1038866.
64. Sözen C, Schenk ST, Boudsocq M, Chardin C, Almeida-Trapp M, Krapp A et al. Wounding and Insect Feeding Trigger Two Independent MAPK Pathways with Distinct Regulation and Kinetics[OPEN]. The Plant Cell. 2020 June 1;32(6):1988–2003.
65. Barros-Rios J, Malvar R, Jung HJ, Santiago R. Cell wall composition as a maize defense mechanism against corn borers. Phytochemistry. 2011;72:365–71.
66. Eklöf JM, Brumer H. The XTH Gene Family: An Update on Enzyme Structure, Function, and Phylogeny in Xyloglucan Remodeling. Plant Physiol. 2010 June;153(1):456–66.
67. Ishida K, Yokoyama R. Reconsidering the function of the xyloglucan endotransglucosylase/hydrolase family. J Plant Res. 2022;135(2):145–56.
68. Dong NQ, Lin HX. Contribution of phenylpropanoid metabolism to plant development and plant–environment interactions. J Integr Plant Biol. 2021;63(1):180–209.
69. Vanholme R, Storme V, Vanholme B, Sundin L, Christensen JH, Goeminne G et al. A Systems Biology View of Responses to Lignin Biosynthesis Perturbations in Arabidopsis. The Plant Cell. 2012 Sept 1;24(9):3506–29.
70. Wang S, Lei C, Wang J, Ma J, Tang S, Wang C, et al. SPL33, encoding an eEF1A-like protein, negatively regulates cell death and defense responses in rice. J Exp Bot. 2017;68(5):899–913.
71. Li Z, Zhang Y, Ren J, Jia F, Zeng H, Li G, et al. Ethylene-responsive factor ERF114 mediates fungal pathogen effector PevD1-induced disease resistance in Arabidopsis thaliana. Mol Plant Pathol. 2022 June;23(6):819–31.

72. Saini S, Sharma I, Pati PK. Versatile roles of brassinosteroid in plants in the context of its homoeostasis, signaling and crosstalks. Front Plant Sci [Internet]. 2015 Nov 4 [cited 2025 July 4];6. Available from: https://www.frontiersin.org/journals/plant-science/articles/10.3389/fpls.2015.00950/full
73. Manghwar H, Hussain A, Ali Q, Liu F. Brassinosteroids (BRs) Role in Plant Development and Coping with Different Stresses. Int J Mol Sci. 2022;23(3):1012.
74. Liao K, Peng YJ, Yuan LB, Dai YS, Chen QF, Yu LJ, et al. Brassinosteroids Antagonize Jasmonate-Activated Plant Defense Responses through BRI1-EMS-SUPPRESSOR1 (BES1)1. Plant Physiol. 2020;182(2):1066–82.
75. Ohnishi T. Recent advances in brassinosteroid biosynthetic pathway: insight into novel brassinosteroid shortcut pathway. J Pestic Sci. 2018;43(3):159–67.
76. Gigolashvili T, Geier M, Ashykhmina N, Frerigmann H, Wulfert S, Krueger S, et al. The Arabidopsis Thylakoid ADP/ATP Carrier TAAC Has an Additional Role in Supplying Plastidic Phosphoadenosine 5'-Phosphosulfate to the Cytosol[W]. Plant Cell. 2012;24(10):4187–204.
77. Zhang H, He Y, Tan X, Xie K, Li L, Hong G, et al. The Dual Effect of the Brassinosteroid Pathway on Rice Black-Streaked Dwarf Virus Infection by Modulating the Peroxidase-Mediated Oxidative Burst and Plant Defense. MPMI. 2019 June;32(6):685–96.
78. Albrecht C, Boutrot F, Segonzac C, Schwessinger B, Gimenez-Ibanez S, Chinchilla D et al. Brassinosteroids inhibit pathogen-associated molecular pattern–triggered immune signaling independent of the receptor kinase BAK1. Proceedings of the National Academy of Sciences. 2012;109(1):303–8.
79. Do THT, Martinoia E, Lee Y, Hwang JU. 2021 update on ATP-binding cassette (ABC) transporters: how they meet the needs of plants. Plant Physiol. 2021;187(4):1876–92.
80. Hwang JU, Song WY, Hong D, Ko D, Yamaoka Y, Jang S, et al. Plant ABC Transporters Enable Many Unique Aspects of a Terrestrial Plant's Lifestyle. Mol Plant. 2016;9(3):338–55.
81. Bienert MD, Siegmund SEG, Drozak A, Trombik T, Bultreys A, Baldwin IT, et al. A pleiotropic drug resistance transporter in *Nicotiana tabacum* is involved in defense against the herbivore *Manduca sexta*. Plant J. 2012;72(5):745–57.
82. Ying W, Wang Y, Wei H, Luo Y, Ma Q, Zhu H, et al. Structure and function of the Arabidopsis ABC transporter ABCB19 in brassinosteroid export. Science. 2024;383(6689):eadj4591.
83. Borkovich KA, Farrelly FW, Finkelstein DB, Taulien J, Lindquist S. hsp82 is an essential protein that is required in higher concentrations for growth of cells at higher temperatures. Mol Cell Biol. 1989 Sept;9(9):3919–30.
84. Edwards JA, Zemska O, Rappleye CA. Discovery of a Role for Hsp82 in Histoplasma Virulence through a Quantitative Screen for Macrophage Lethality □. Infect Immun. 2011;79(8):3348–57.
85. Abdul Malik NA, Kumar IS, Nadarajah K. Elicitor and Receptor Molecules: Orchestrators of Plant Defense and Immunity. Int J Mol Sci. 2020;21(3):963.

86. Zhang H, Zhang F, Yu Y, Feng L, Jia J, Liu B, et al. A Comprehensive Online Database for Exploring ~20,000 Public Arabidopsis RNA-Seq Libraries. Mol Plant. 2020 Sept;7(9):1231–3.
87. Koch K. Sucrose metabolism: regulatory mechanisms and pivotal roles in sugar sensing and plant development. Current Opinion in Plant Biology. 2004 June 1;7(3):235–46.
88. Thines E, Weber RWS, Talbot NJ. MAP Kinase and Protein Kinase A–Dependent Mobilization of Triacylglycerol and Glycogen during Appressorium Turgor Generation by Magnaporthe grisea. The Plant Cell. 2000 Sept 1;12(9):1703–18.
89. Dixon DP, Skipsey M, Edwards R. Roles for glutathione transferases in plant secondary metabolism. Phytochemistry. 2010;71(4):338–50.
90. Moons A. Regulatory and Functional Interactions of Plant Growth Regulators and Plant Glutathione S-Transferases (GSTs). In: Litwack G, editor. Vitamins & Hormones [Internet]. Academic Press; 2005 [cited 2025 Jan 5]. pp. 155–202. (Plant Hormones; vol. 72). Available from: https://www.sciencedirect.com/science/article/pii/S0083672905720057
91. Park HL, Seo DH, Lee HY, Bakshi A, Park C, Chien YC et al. Ethylene-triggered subcellular trafficking of CTR1 enhances the response to ethylene gas. Nat Commun. 2023;14(1).
92. Castellano MM, Muñoz A, Okeke IC, Novo-Uzal E, Toribio R, Mangano S. The role of the co-chaperone HOP in plant homeostasis during development and stress. J Exp Bot. 2024;75(14):4274–86.
93. Muhammad T, Yang T, Wang B, Yang H, Tuerdiyusufu D, Wang J, et al. Comprehensive genomic characterization and expression analysis of calreticulin gene family in tomato. Front Plant Sci. 2024;15:1397765.
94. Kumar A, Krausko M, Jásik J. SYNAPTOTAGMIN 4 is expressed mainly in the phloem and participates in abiotic stress tolerance in Arabidopsis. Front Plant Sci [Internet]. 2024 July 1 [cited 2025 July 15];15. Available from: https://www.frontiersin.org/journals/plant-science/articles/10.3389/fpls.2024.1363555/full
95. Shelomi M, Lin SS, Liu LY. Transcriptome and microbiome of coconut rhinoceros beetle (Oryctes rhinoceros) larvae. BMC Genomics. 2019;20(1):957.
96. Giovino A, Bertolini E, Fileccia V, Al Hassan M, Labra M, Martinelli F. Transcriptome analysis of Phoenix canariensis Chabaud in response to Rhynchophorus ferrugineus Olivier attacks. Front Plant Sci. 2015;6:817.
97. Shalini KV, Manjunatha S, Lebrun P, Berger A, Baudouin L, Pirany N, et al. Identification of molecular markers associated with mite resistance in coconut (Cocos nucifera L). Genome. 2007;50(1):35–42.
98. Huq MA, Akter S, Nou IS, Kim HT, Jung YJ, Kang. Identification of functional SNPs in genes and their effects on plant phenotypes. J Plant Biotechnol. 2016;43(1):1–11.
99. Korsa F. Effects of Functional Single Nucleotide Polymorphisms on Plant Phenotypes. Archives Crop Sci. 2022;5(2):185–92.
100. Kwon JS, Lee J, Shilpha J, Jang H, Kang WH. The landscape of sequence variations between resistant and susceptible hot peppers to predict functional candidate genes against bacterial wilt disease. BMC Plant Biol. 2024;24(1):1036.

101. Yates CM, Sternberg MJE. The effects of non-synonymous single nucleotide polymorphisms (nsSNPs) on protein-protein interactions. J Mol Biol. 2013;425(21):3949–63.
102. Stevanato P, Trebbi D, Panella L, Richardson K, Broccanello C, Pakish L et al. Identification and Validation of a SNP Marker Linked to the Gene HsBvm-1 for Nematode Resistance in Sugar Beet. Plant Mol Biol Rep. 2015 June 1;33(3):474–9.
103. Klees S, Heinrich F, Schmitt AO, Gültas M. agReg-SNPdb: A Database of Regulatory SNPs for Agricultural Animal Species. Biology (Basel). 2021;10(8):790.
104. Zhu P, Schon M, Questa J, Nodine M, Dean C. Causal role of a promoter polymorphism in natural variation of the *Arabidopsis* floral repressor gene *FLC*. Curr Biol. 2023;33(20):4381–e43913.
105. Das MK, Dai HK. A survey of DNA motif finding algorithms. BMC Bioinformatics. 2007;8(7):S21.
106. Korhonen JH, Palin K, Taipale J, Ukkonen E. Fast motif matching revisited: high-order PWMs, SNPs and indels. Bioinformatics. 2017;33(4):514–21.
107. Wu X, Xia M, Su P, Zhang Y, Tu L, Zhao H, et al. MYB transcription factors in plants: A comprehensive review of their discovery, structure, classification, functional diversity and regulatory mechanism. Int J Biol Macromol. 2024;282:136652.
108. Xu T, Mitra R, Tan D, Li Z, Zhou C, Chen T, et al. Utilization of gene manipulation system for advancing the biotechnological potential of halophiles: A review. Biotechnol Adv. 2024;70:108302.
109. Bartlett MS. Determinants of transcription initiation by archaeal RNA polymerase. Curr Opin Microbiol. 2005;8(6):677–84.
110. Patikoglou GA, Kim JL, Sun L, Yang SH, Kodadek T, Burley SK. TATA element recognition by the TATA box-binding protein has been conserved throughout evolution. Genes Dev. 1999;13(24):3217–30.
111. Godbey WT. Chapter 4 - Genes: the blueprints for proteins. In: Godbey WT, editor. Biotechnology and its Applications (Second Edition) [Internet]. Academic Press; 2022 [cited 2025 Jan 17]. pp. 73–115. Available from: https://www.sciencedirect.com/science/article/pii/B9780128177266000046
112. Xu M, Gonzalez-Hurtado E, Martinez E. Core promoter-specific gene regulation: TATA box selectivity and Initiator-dependent bi-directionality of serum response factor-activated transcription. Biochim Biophys Acta. 2016;1859(4):553–63.
113. Baker EK, El-Osta A. The rise of DNA methylation and the importance of chromatin on multidrug resistance in cancer. Exp Cell Res. 2003;290(2):177–94.
114. Anjum KH, Nadeem A, Javed M, Ahmad HI, Riaz A, Shehzad W, et al. Genomic and Computational Analysis of Novel SNPs in TNP1 Gene Promoter Region of Bos indicus Breeding Bulls. Genet Res (Camb). 2022;2022:9452234.
115. Maston GA, Evans SK, Green MR. Transcriptional regulatory elements in the human genome. Annu Rev Genomics Hum Genet. 2006;7:29–59.
116. Hufford MB, Xu X, van Heerwaarden J, Pyhäjärvi T, Chia JM, Cartwright RA et al. Comparative population genomics of maize domestication and improvement. Nat Genet 2012 June 3;44(7):808–11.

117. Istanbuli T, Nassar AE, Abd El-Maksoud MM, Tawkaz S, Alsamman AM, Hamwieh A. Genome-wide association study reveals SNP markers controlling drought tolerance and related agronomic traits in chickpea across multiple environments. Front Plant Sci [Internet]. 2024 Mar 8 [cited 2025 Dec 11];15. Available from: https://www.frontiersin.org/journals/plant-science/articles/10.3389/fpls.2024.1260690/full

Figures

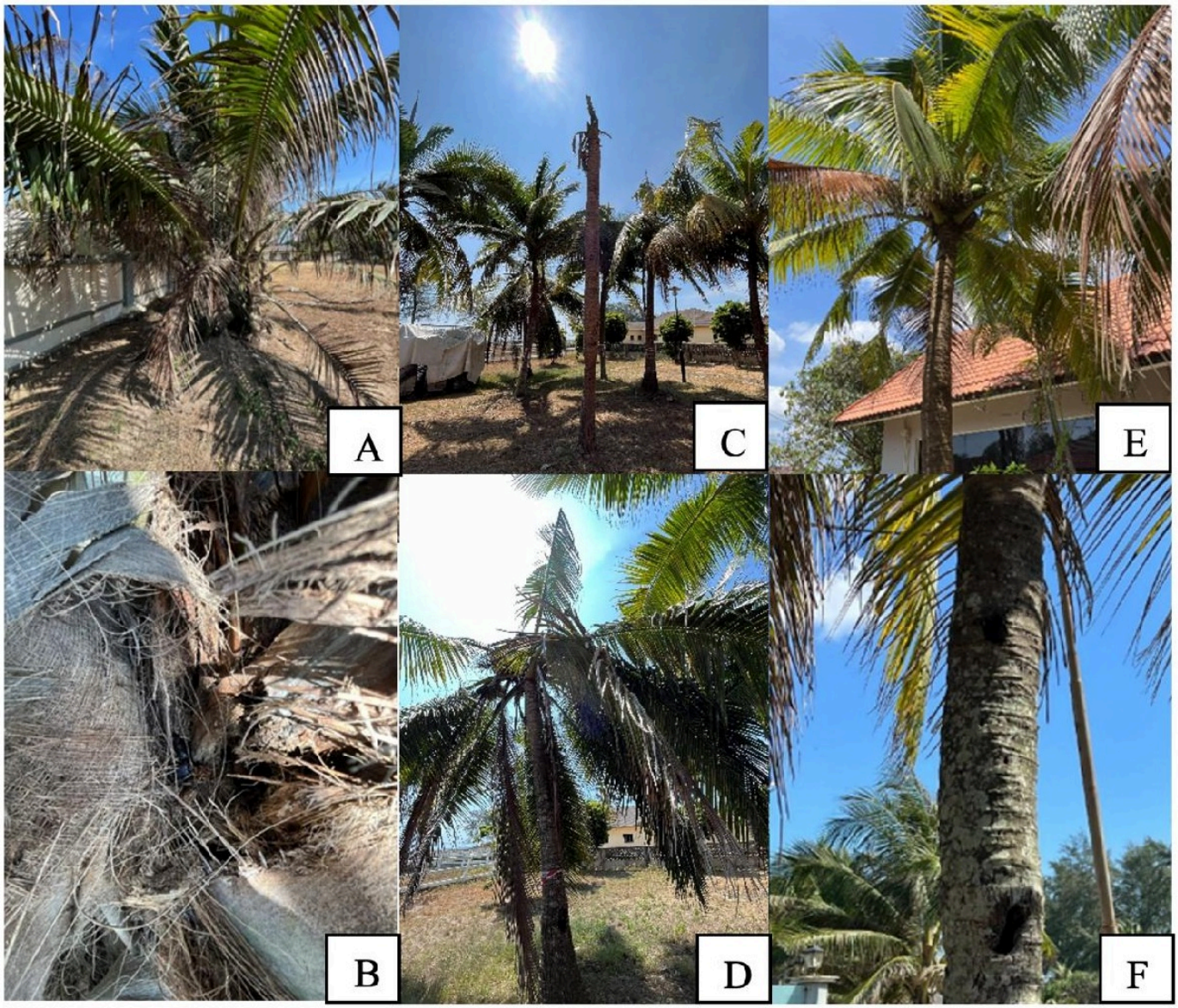

Figure 1

Observation on external damage due to high level of RPW infestation in three different varieties in the same coconut field. Damage shown on the Pandan variety with collapsed crown and dried fronds (A)

and chewed fibers with active feeding of RPW adult (B). MT variety with final stage of RPW infestation without the presence of any apical shoot, crown and fronds (C) and damaged crown and collapsed frond (D). Healthy MYD palm with few dried leaves and healthy apical shoots (E) and MYD palm with the holes in the trunk showing the RPW infestation but remain healthy (F).

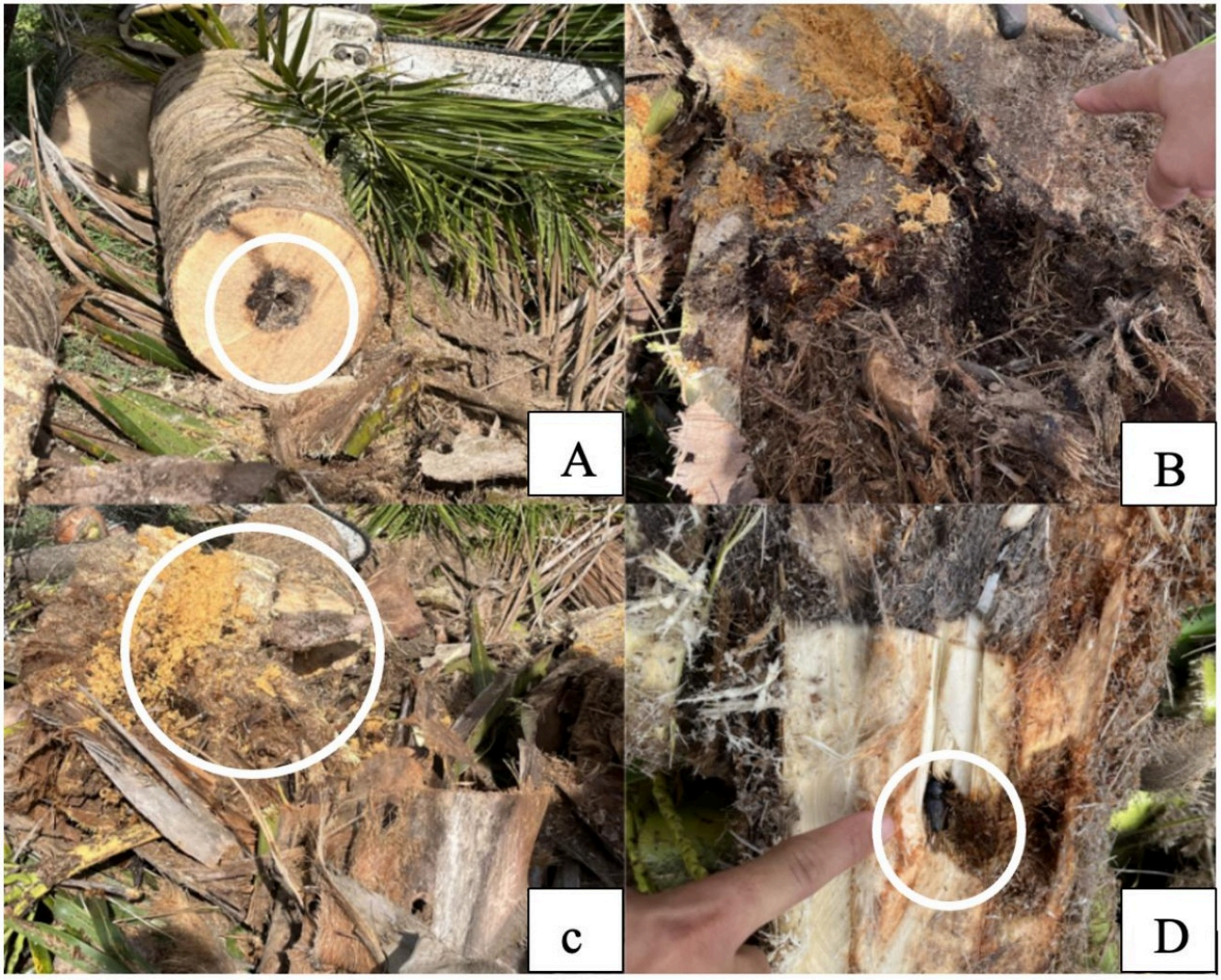

Figure 2

Observation on Internal damage of the Malayan Tall variety due to RPW infestation. The tunnel made through the trunk as RPW moves from the bottom of the palm towards the cabbage in Malayan Tall variety (A); the chewed fiber throughout the tunnel created by the RPW showing severely damaged cabbage of the palm with black coloration, oozing and foul smell (B); completely chewed fiber of the cabbage of the palm (C) and active feeding RPW in the cabbage of the palm with the surrounding area of the feeding to be dark and has the oozing sap (D).

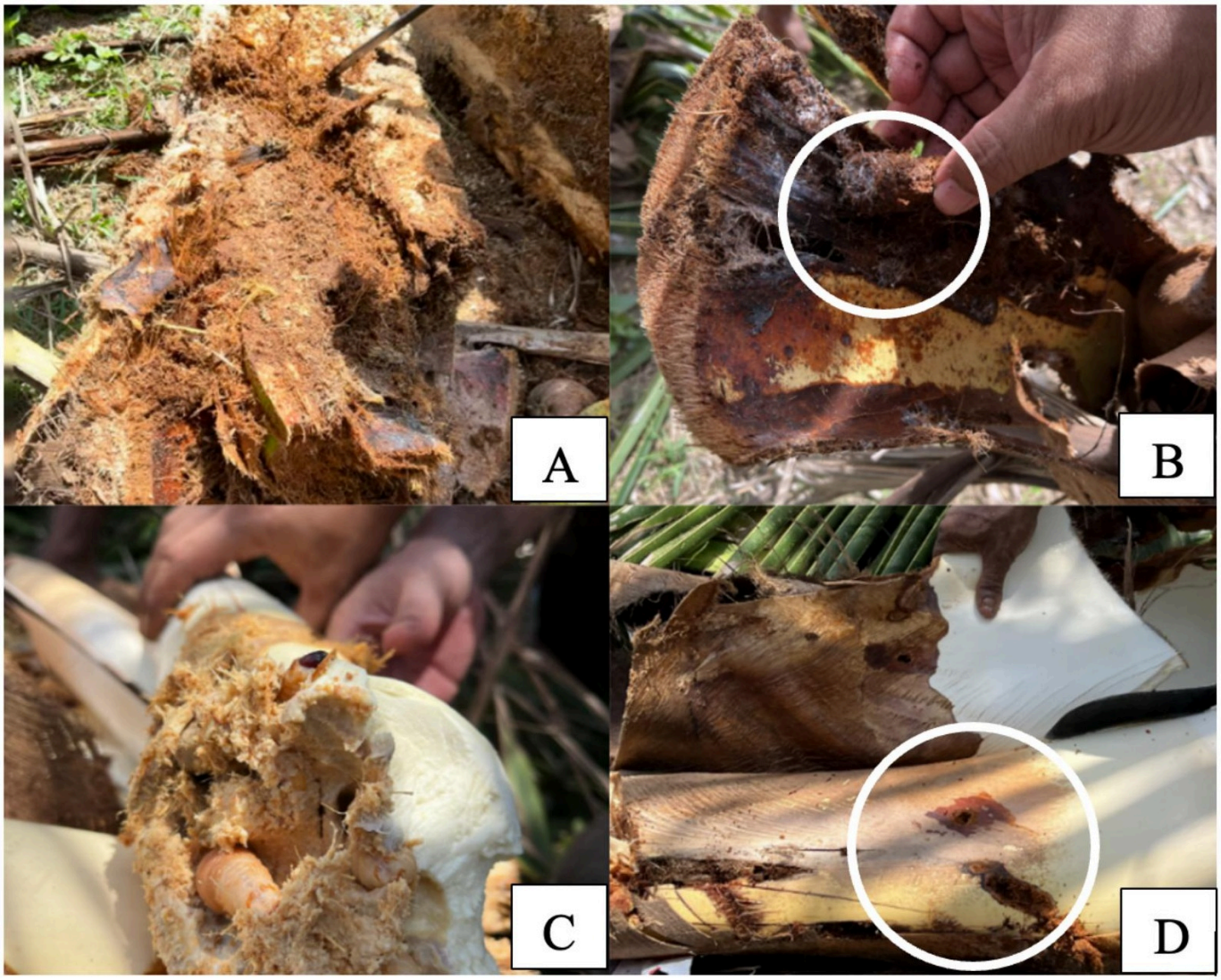

Figure 3

Observation on Internal damage due to RPW infestation in Pandan Variety. The cabbage fiber of the palm fully chewed and destroyed by RPW larvae (A); the presence of pupal in the cocoon in the petiole of the palm which shows the deposition of the egg by adult RPW in the petiole of the palm (B); the presence of RPW larvae actively feeding in the internal cabbage of the palm (C) and the holes made by RPW larvae in the cabbage of the palm (D).

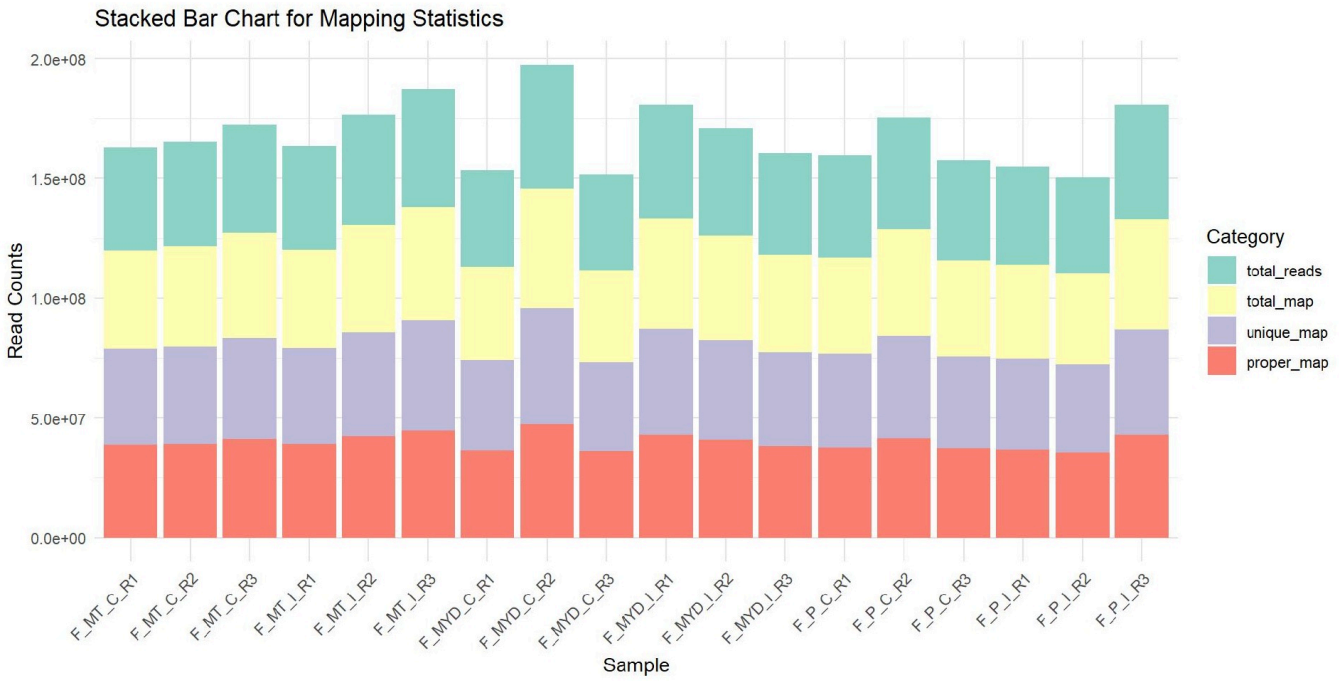

Figure 4

Horizontal Stacked Bar Chart displaying mapping statistics for each sample. The total length of each bar represents the total reads (total reads), with stacked segments corresponding to the mapping categories: total map, unique map, and proper map. The chart visualizes the distribution of mapped reads across different categories for each sample, with the y-axis representing the read count and the x-axis representing individual samples.

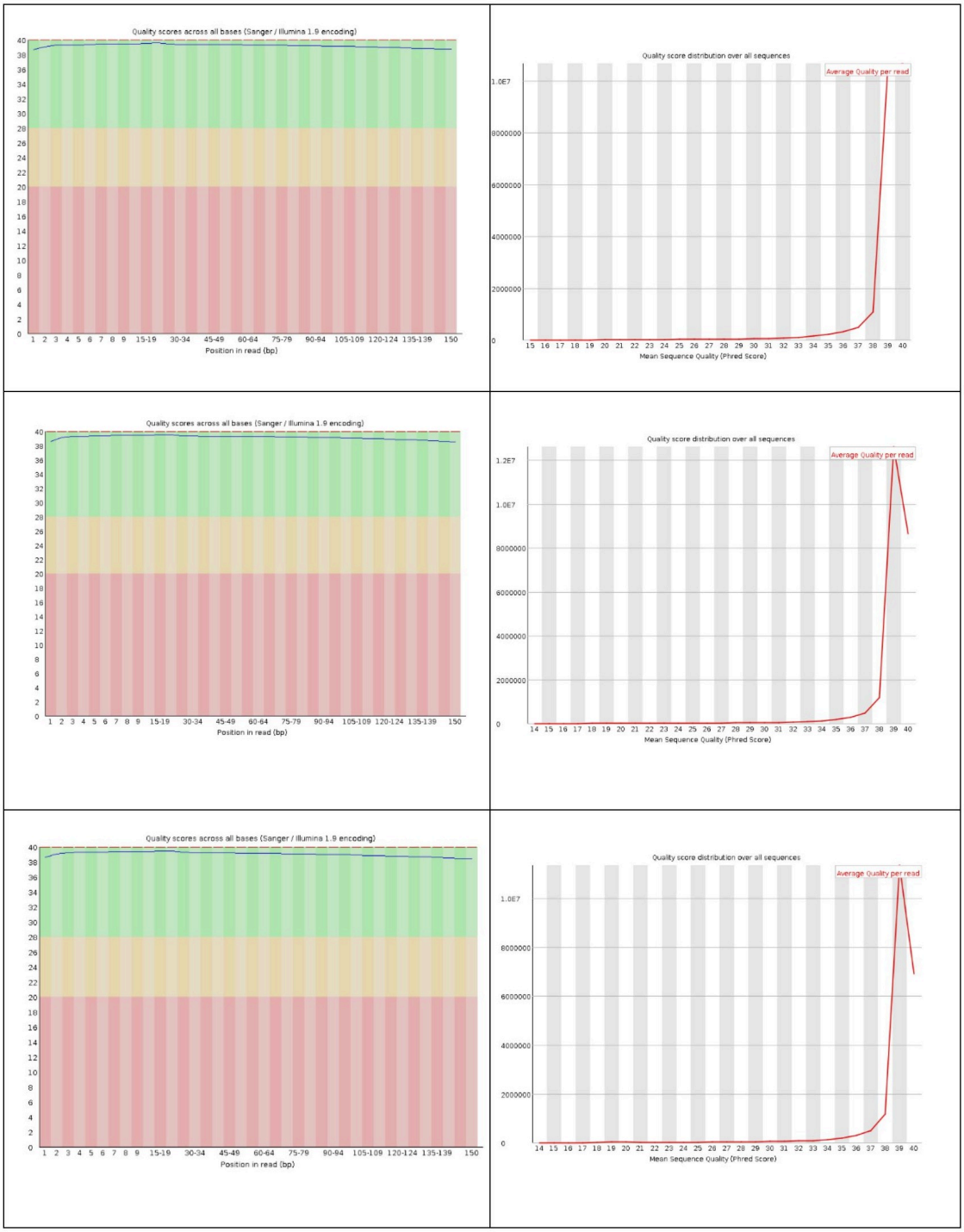

Figure 5

Per base sequence quality of samples generated by FastQC. Yellow boxes demonstrate base-calling quality scores across the sample from replicate 1, replicate 2, and replicate 3. The Phred score according to the number of sequences is presented at the right-hand side of each replicate.

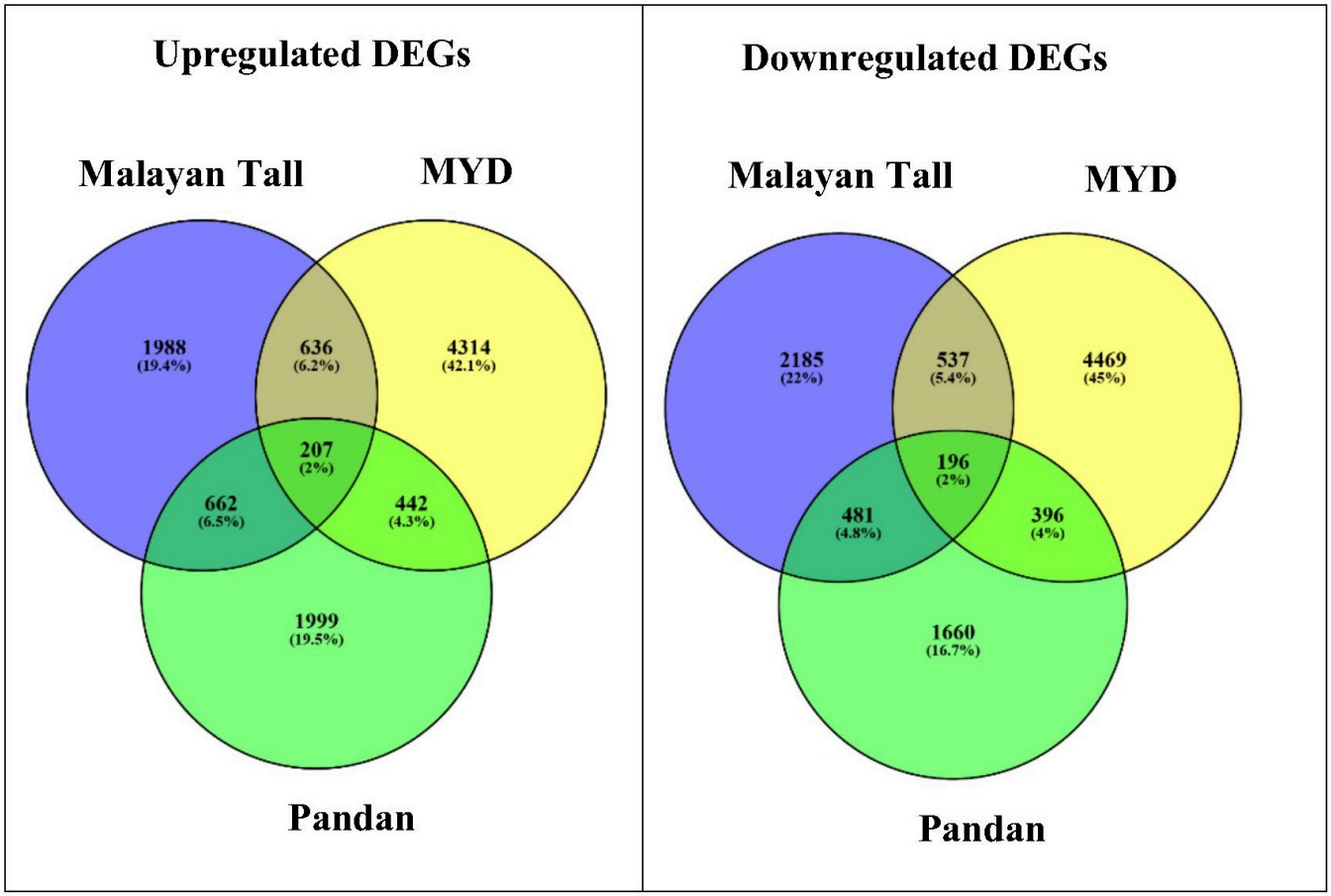

Figure 6

Venn diagram of upregulated and downregulated DEGs among the three varieties, which are Pandan, MYD, and Malayan Tall.

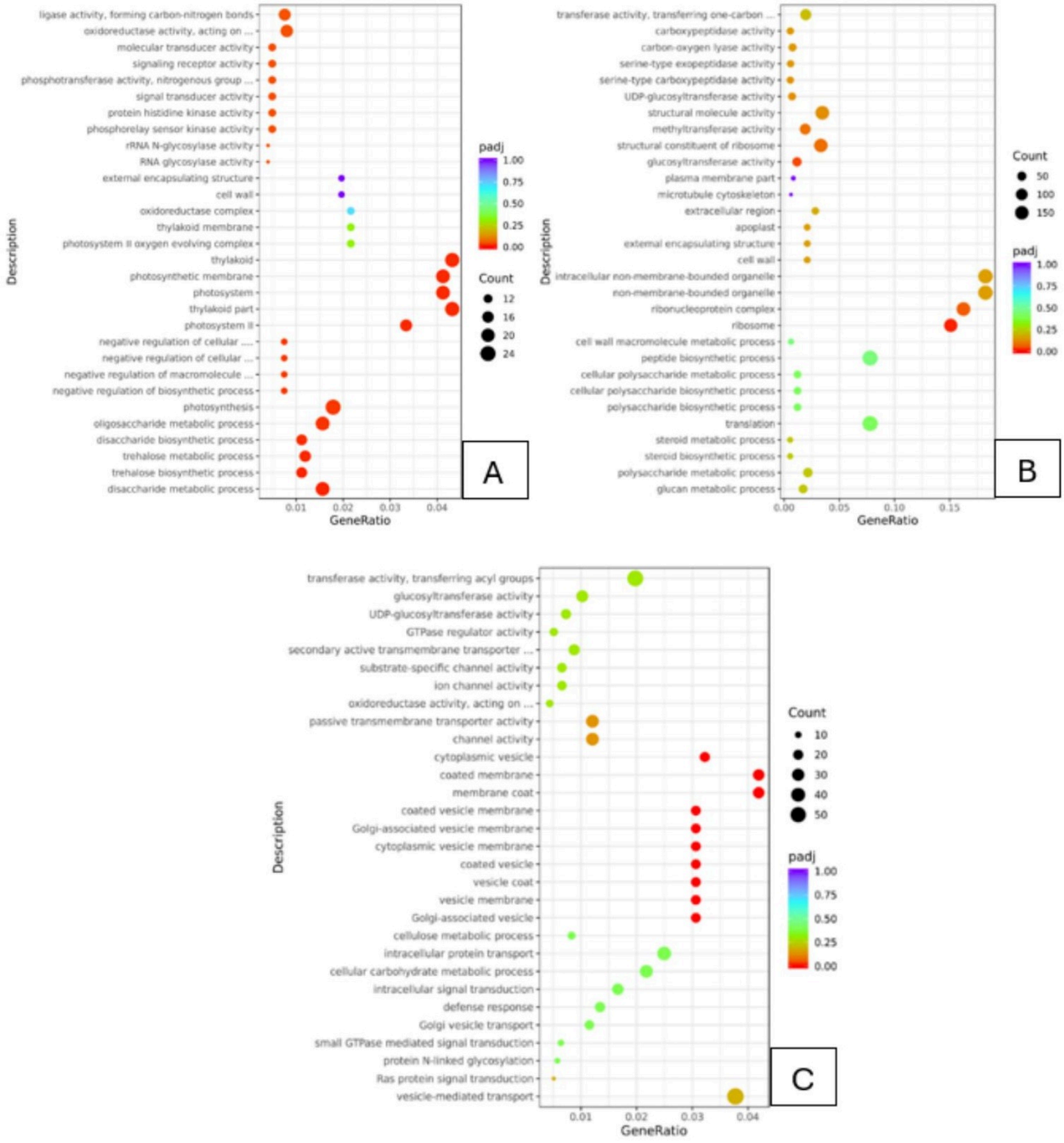

Figure 7

Dot plots of Gene Ontology (GO) enrichment analysis for three coconut varieties: (A) Pandan, (B) (MYD), and (C) (MT). Differentially expressed genes (DEGs) in each variety were categorized into Biological Process (BP), Cellular Component (CC), and Molecular Function (MF) terms. The x-axis denotes the GeneRatio, while the y-axis lists enriched GO terms. The size of each dot corresponds to the number of

genes associated with that term, and the color gradient indicates the adjusted *p*-value (*padj*), with red representing highly significant terms and purple/blue representing less significant terms.

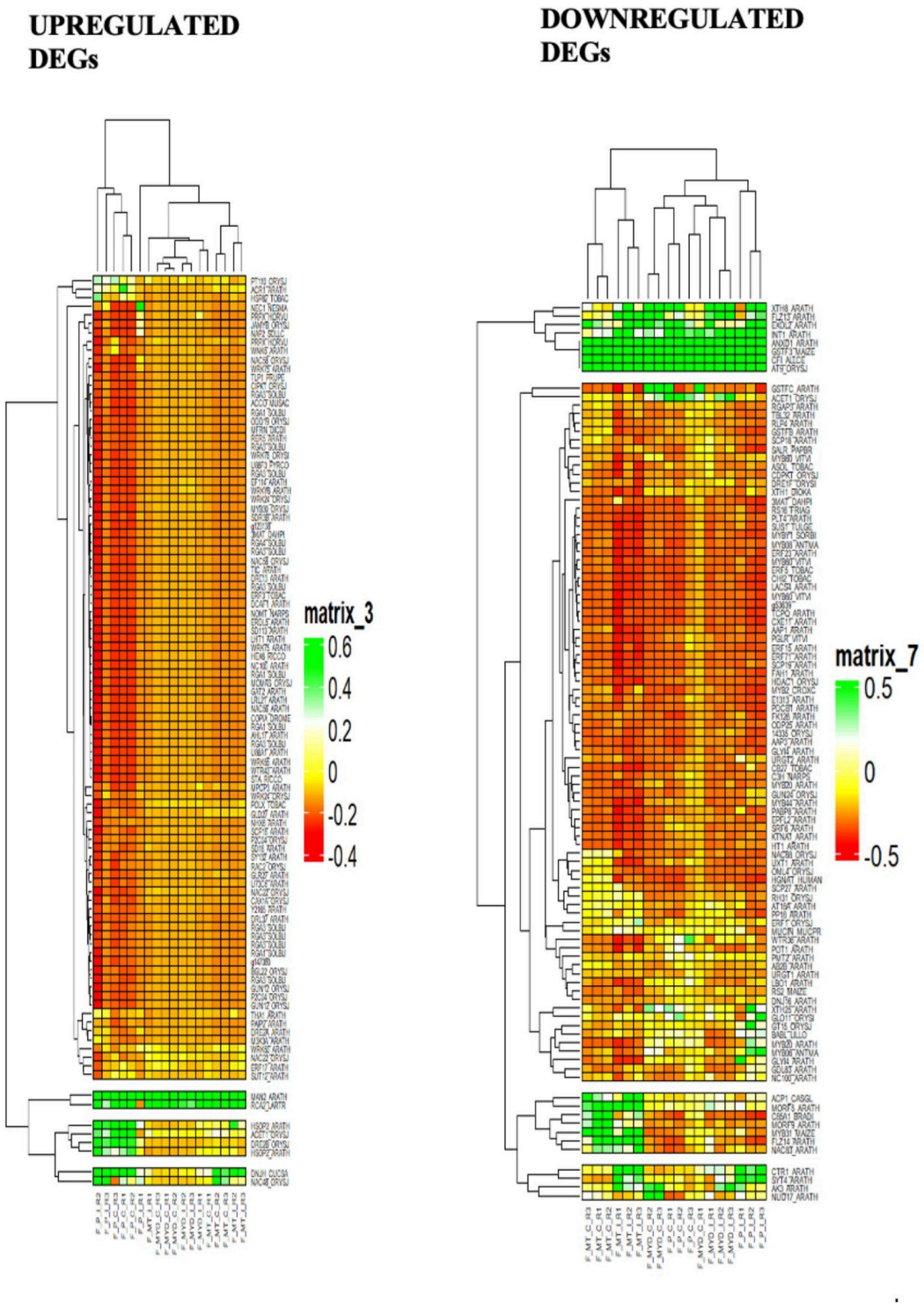

Figure 8

Heatmap of top 100 upregulated and top 100 downregulated differentially expressed genes in biological samples from control and infested fields of the three varieties. The color intensity of each plot is based

on the FPKM value of the gene expression of the DEGs of the Pandan, MYD, and Malayan Tall varieties compared to the control group, respectively.

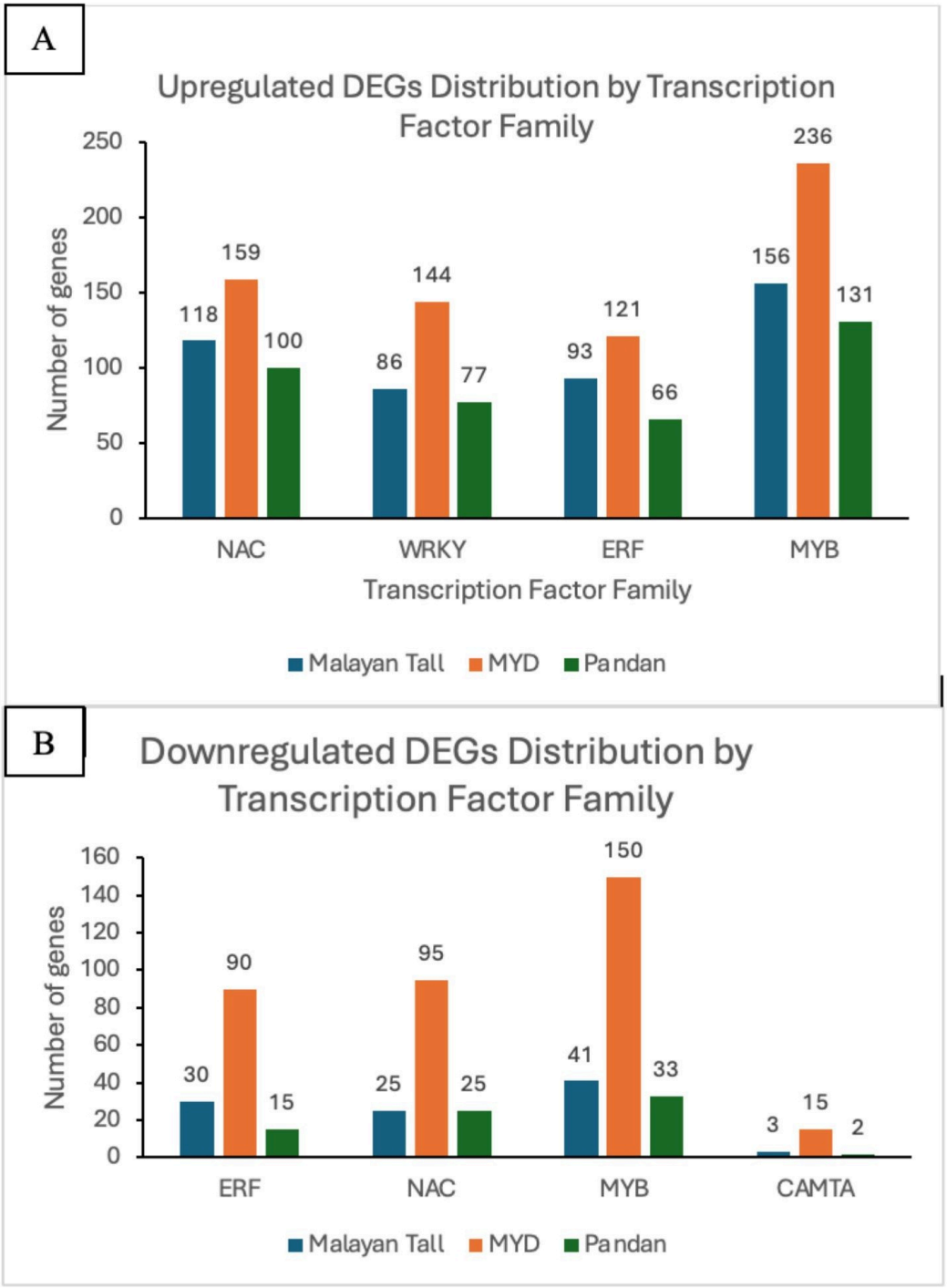

Figure 9

Bar charts of distribution of differentially expressed genes (DEGs) across three varieties of coconut (Malayan Tall, MYD and Pandan). Greater number of genes belonging to the NAC, WRKY, ERF and MYB families of transcription factor were upregulated in the resistant MYD variety compared to the

susceptible varieties (Malayan Tall and Pandan) (A) and greater number of genes belonging to the ERF, NAC, MYB and CAMTA families of transcription factor were downregulated in the resistant MYD variety compared to the susceptible varieties (Malayan Tall and Pandan) (B).

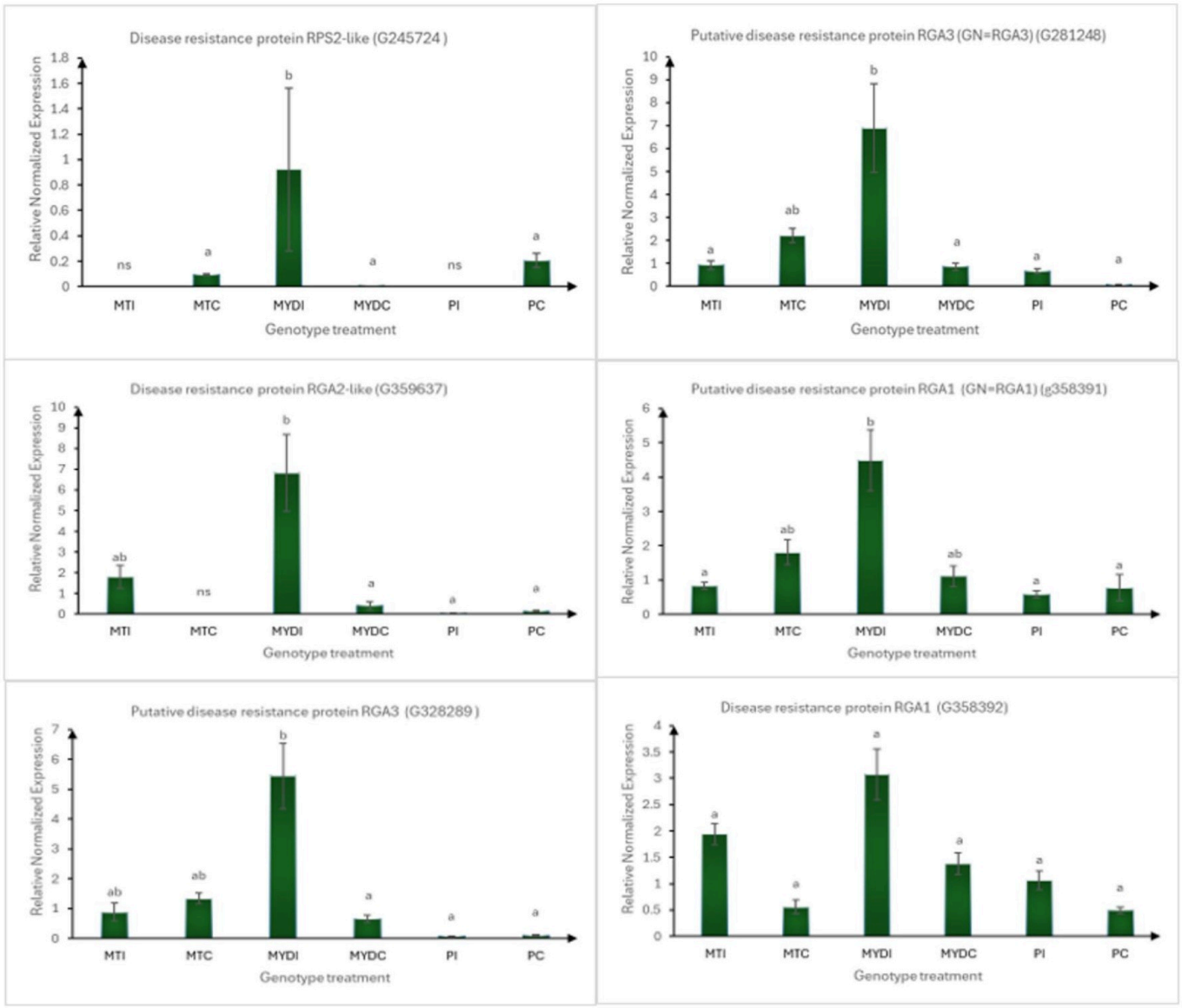

Figure 10

Validation of RNA-seq data using quantitative polymerase chain reaction (qPCR). The analysis was performed on Malayan Tall, Pandan and MYD RPW-infested and non-infested field as control samples. The expression profile of disease resistance protein RPS2-like (G245724) (A); putative disease resistance protein RGA3 (G2812948) (B); putative disease resistance protein RGA2 (G359637) (C), putative disease resistance protein RGA1 (G358391) (D) and putative disease resistance protein RGA3 (G2812948) (E) showed significant higher expression in the MYDI infested biological sample and only one putative disease resistance protein RGA1 (G358392) (F) is not significantly different from others. qPCR data are expressed as fold change mean, with error bars representing the standard error of the

mean (SEM) from three biological replicates per group**.** Each biological replicate consists of three technical replicates to ensure accurate quantification.

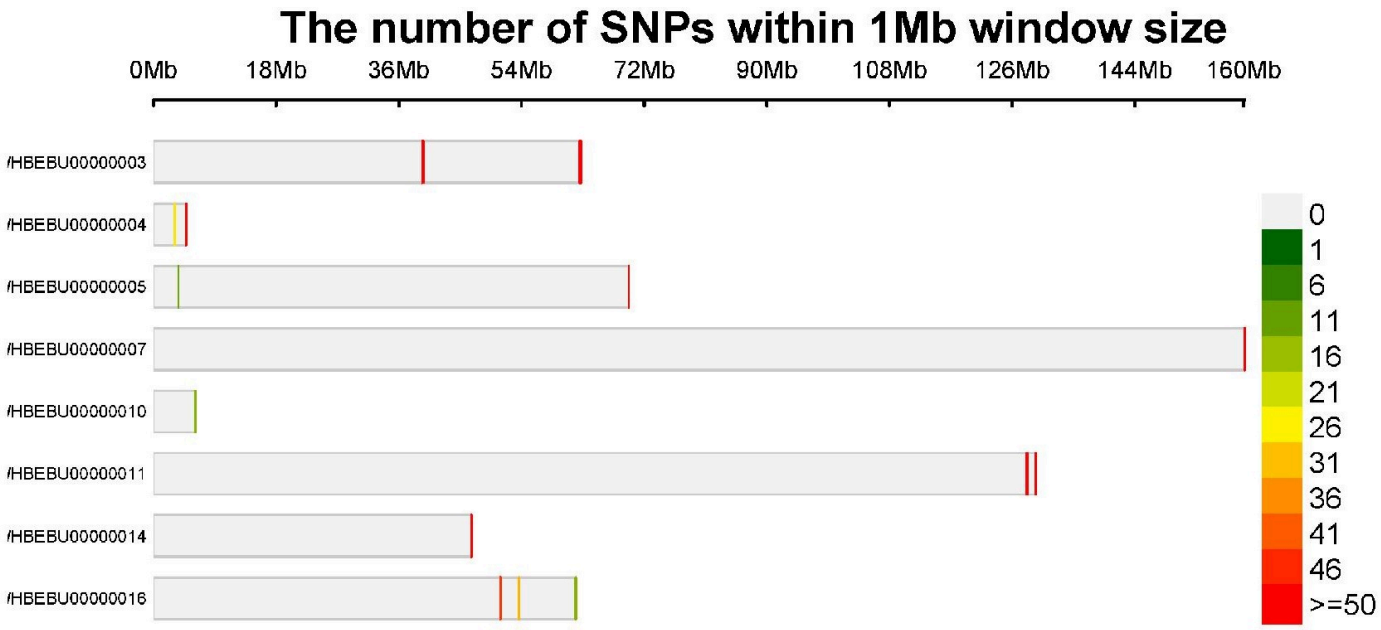

Figure 11

SNP Density Across the chromosomes. This figure shows the SNP density distribution across the chromosomes with 1Mb window size, visualizing the concentration of SNP variants per chromosome. The plot highlights regions with varying SNP densities, illustrating the distribution pattern of the SNP variants identified in the dataset.

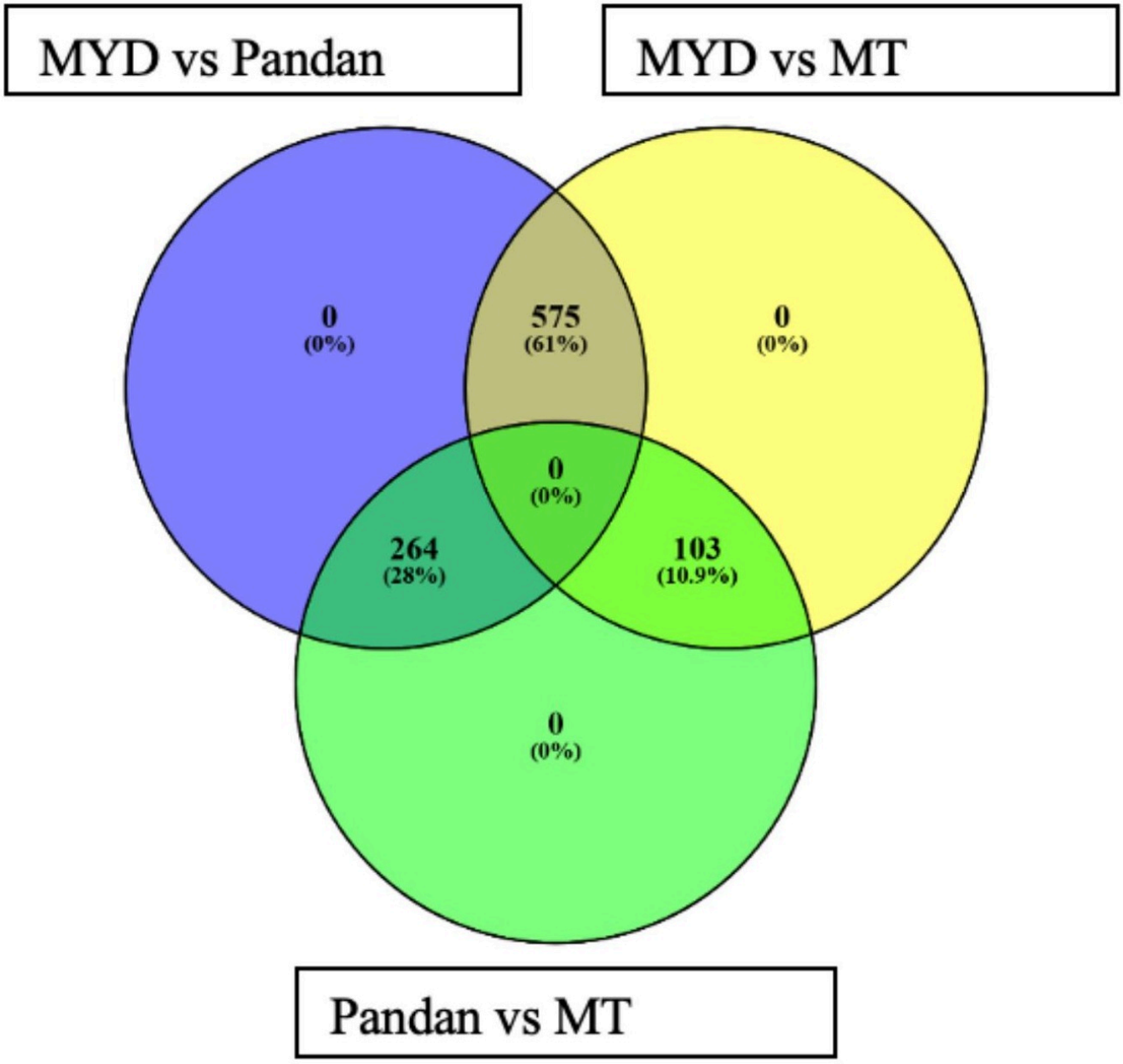

Figure 12

Venn Diagram of SNP Variant Overlaps Among Three Coconut Pairwise Comparison Groups. This figure illustrates the overlap of SNP variants identified in pairwise comparisons among the three groups: Group 1 (MYD vs. Pandan), Group 2 (MYD vs. MT), and Group 3 (Pandan vs. MT). Each circle represents the set of SNP variants identified within a specific group, and the intersections indicate shared variants among the groups. This visualization highlights the unique and common genetic variations across the three pairwise comparisons.

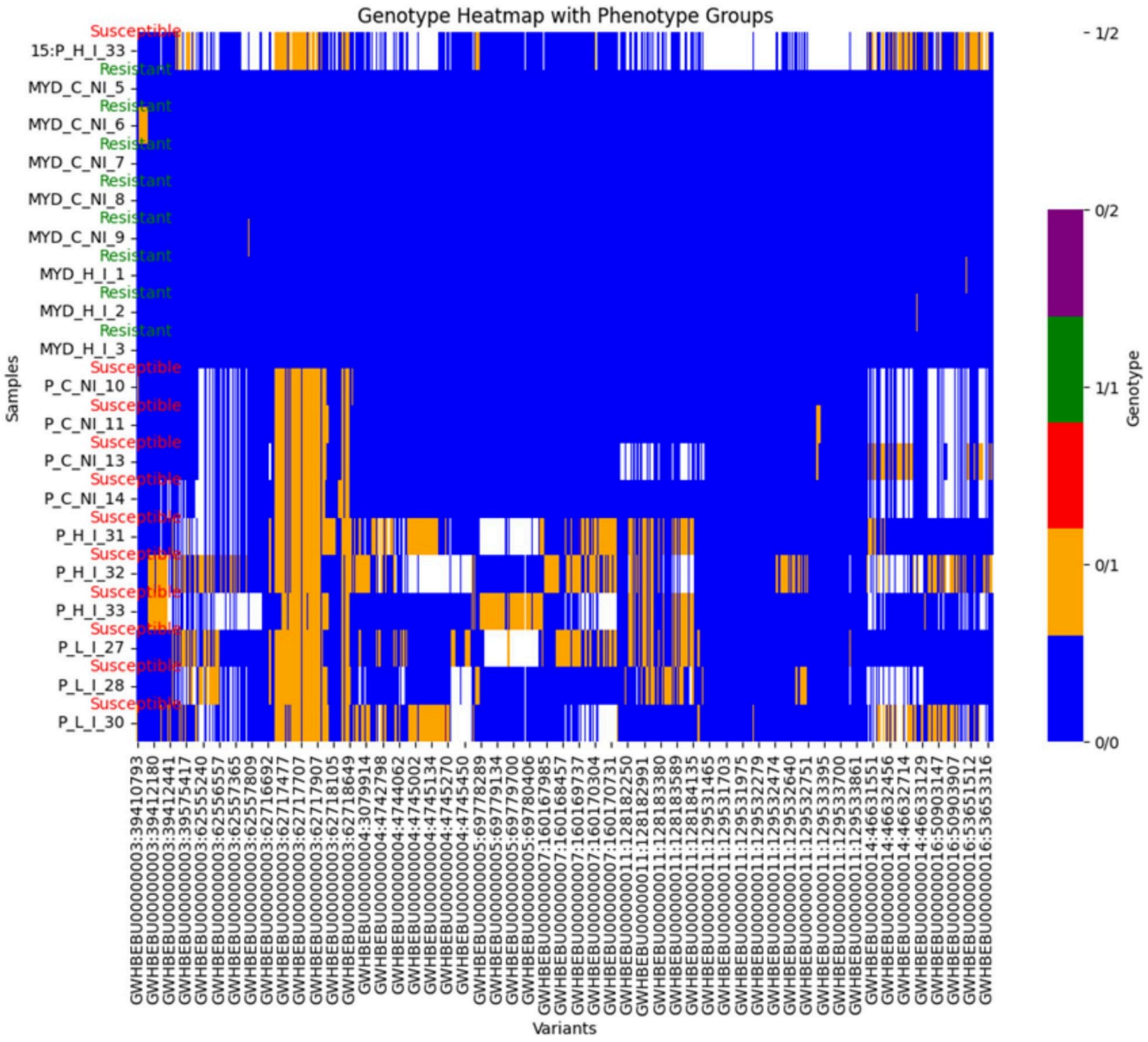

Figure 13

Heatmap of Genotype Comparison Between Resistant (MYD) and Susceptible (Pandan) Coconut Varieties. The heatmap displays the genotype differences between MYD (resistant) and Pandan (susceptible) varieties, with each row representing a specific SNP and each column corresponding to an individual sample. The color intensity indicates the genotype, with distinct colours representing varying alleles at each SNP position.

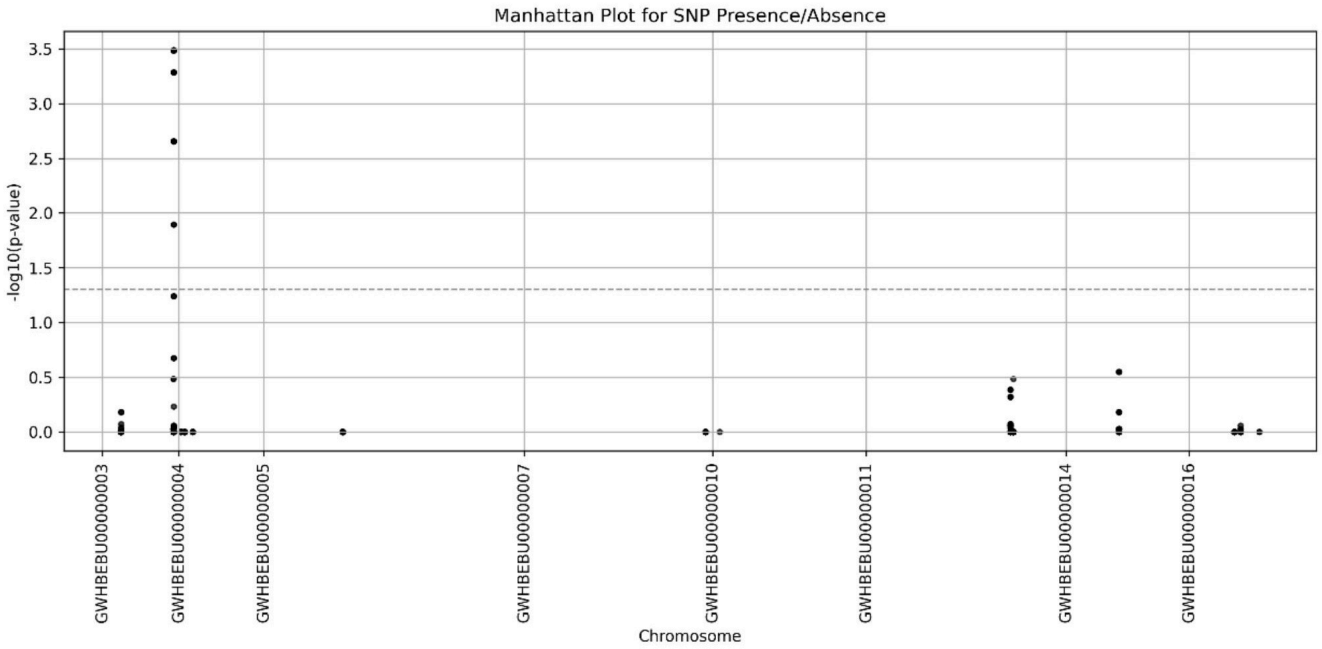

Figure 14

Manhattan plot for the presence of significant SNP identified in the Pandan (Susceptible variety) using Fisher's Exact Test and FDR. This Manhattan plot visualizes the presence or absence of SNPs cross different chromosomes. The x-axis represents chromosome identifiers, while the y-axis shows the -log10(p-value), indicating the significance of SNP associations. Each point corresponds to an SNP, with higher values suggesting stronger statistical significance. Notably, chromosome GWHHEBU0000003 exhibits the most significant SNPs, while other chromosomes show fewer or less significant variants. The dashed line represents a potential significance threshold where only 4 SNPs passed the significant threshold.

Supplementary Files

This is a list of supplementary files associated with this preprint. Click to download.

- Additionalfile12and3.docx
- Additionalfile4QCstatistic.xlsx
- Additionalfile5GosignificantenrichedinPandan.xlsx
- Additionalfile6GosignificantenrichedinMYD.xlsx
- Additionalfile7osignificantenrichedinMT.xlsx